Characterization of the early events leading to totipotency in an Arabidopsis protoplast liquid culture by temporal transcript profiling

M-Christine M.-C. Chupeau, Fabienne F. Granier, Olivier O. Pichon, Jean-Pierre J.-P. Renou, Valérie Gaudin, Yves Y. Chupeau

The Plant Cell, Vol. 25: 2444–2463, July 2013, www.plantcell.org

LARGE-SCALE BIOLOGY ARTICLE

Characterization of the Early Events Leading to Totipotency in an *Arabidopsis* Protoplast Liquid Culture by Temporal Transcript Profiling[W][OPEN]

Marie-Christine Chupeau,[a] Fabienne Granier,[a] Olivier Pichon,[b,2] Jean-Pierre Renou,[b,3] Valérie Gaudin,[a,1] and Yves Chupeau[a,1,4]

[a] Institut National de la Recherche Agronomique, Unité Mixte de Recherche 1318–AgroParisTech, Institut Jean-Pierre Bourgin, Institut National de la Recherche Agronomique–Centre de Versailles-Grignon, F-78026 Versailles cedex, France
[b] Institut National de la Recherche Agronomique, Unité Mixte de Recherche 1165, Unité Mixte de Recherche en Génomique Végétale, F-91057 Évry cedex 2, France

The molecular mechanisms underlying plant cell totipotency are largely unknown. Here, we present a protocol for the efficient regeneration of plants from *Arabidopsis thaliana* protoplasts. The specific liquid medium used in our study leads to a high rate of reentry into the cell cycle of most cell types, providing a powerful system to study dedifferentiation/regeneration processes in independent somatic cells. To identify the early events in the establishment of totipotency, we monitored the genome-wide transcript profiles of plantlets and protoplast-derived cells (PdCs) during the first week of culture. Plant cells rapidly dedifferentiated. Then, we observed the reinitiation and reorientation of protein synthesis, accompanied by the reinitiation of cell division and de novo cell wall synthesis. Marked changes in the expression of chromatin-associated genes, especially of those in the histone variant family, were observed during protoplast culture. Surprisingly, the epigenetic status of PdCs and well-established cell cultures differed, with PdCs exhibiting rare reactivated transposons and epigenetic changes. The differentially expressed genes identified in this study are interesting candidates for investigating the molecular mechanisms underlying plant cell plasticity and totipotency. One of these genes, the plant-specific transcription factor *ABERRANT LATERAL ROOT FORMATION4*, is required for the initiation of protoplast division.

INTRODUCTION

Multiple regeneration mechanisms, based on various progenitor cell sources, exist in plants. Most of these were identified through the development of in vitro tissue culture techniques and were subsequently used in plant biotechnology applications (Vasil, 2008). For over 50 years, it has been known that applications of auxin and cytokinin phytohormones can chemically induce plant cell reprogramming (Skoog and Miller, 1957). However, the underlying mechanisms are poorly understood. Recently, based on a study using in vitro *Arabidopsis thaliana* root segments, it was proposed that meristem formation arises from *trans*-differentiation of a specific population of starting cells that are equivalent to adult stem cells and that regeneration occurs by differentiation of these progenitor cells (Atta et al., 2009; Sugimoto et al., 2010, 2011). In root segments, the controlled asymmetric division of specific pericycle cells (De Smet et al., 2008) is closely linked to cell fate respecification in lateral root founder cells (Vanneste et al., 2005). One of the major limits to understanding the initial molecular reprogramming events that lead to totipotency arises from the complexity of the model explants.

Besides *trans*-differentiation, dedifferentiation is another developmental switch that can provide progenitor cell sources for the regeneration of multicellular organisms. Dedifferentiation is observed after protoplasting, the enzymatic removal of the plant cell wall. Indeed, in appropriate culture conditions, protoplast-derived cells (PdCs) proliferate and form microcalli, which can undergo regeneration (Nitsch and Oyama, 1971; Takebe et al., 1971). Once it was established that regeneration could occur from single somatic dedifferentiated cells, this regeneration process was applied to a large range of plant species (Davey et al., 2005). The plasticity of plant protoplasts is reminiscent of the totipotency of animal stem cells (González et al., 2011; Jopling et al., 2011). In some species, such as tobacco (*Nicotiana tabacum*), almost 100% of leaf protoplasts yielded cell colonies and ultimately plants (Bourgin et al., 1979), suggesting that dividing protoplasts can be obtained from various differentiated cells. To attain high regeneration rates, it was recommended that young and nonstressed tissues be used for protoplast isolation (Chupeau et al., 1974) and that plant growth conditions be adjusted to avoid premature cell death (Horii and Marubashi, 2005).

[1] These authors contributed equally to this work.
[2] Current address: Service de Génétique Médicale Institut de Biologie, Centre Hospitalier Universitaire, 9 quai Moncousu, F-44093 Nantes, France.
[3] Current address: Institut de Recherche en Horticulture et Semences, 42 rue Georges Morel, F-49045 Angers, France.
[4] Address correspondence to yves.chupeau@versailles.inra.fr.
The author responsible for distribution of materials integral to the findings presented in this article in accordance with the policy described in the Instructions for Authors (www.plantcell.org) is: Yves Chupeau (yves.chupeau@versailles.inra.fr).
[W] Online version contains Web-only data.
[OPEN] Articles can be viewed online without a subscription.
www.plantcell.org/cgi/doi/10.1105/tpc.113.109538

The early developmental stages initiated in protoplasts are accompanied by large-scale chromatin remodeling (Zhao et al., 2001; Tessadori et al., 2007) and by major transcriptional changes (Xiao et al., 2012). Thus, plant protoplasts offer an alternative model system to decipher the molecular basis underlying dedifferentiation and cell reprogramming prior to regeneration.

The model plant *Arabidopsis* offers various large-scale and genome-wide analysis tools (Atias et al., 2009). However, *Arabidopsis* protoplasts have been mainly used in short-term studies based on transient expression experiments (Yoo et al., 2007; Zhai et al., 2009). Indeed, *Arabidopsis* protoplast culture is known to be technically challenging. Although plants can regenerate from calli derived from *Arabidopsis* protoplasts embedded in gelified medium (Damm and Willmitzer, 1988), the regeneration rate is low, with only 1 to 10% forming cell colonies (Masson and Paszkowski, 1992; Dovzhenko et al., 2003). Furthermore, the use of gelified medium prevented the easy collection of PdCs for biochemical analyses and other studies aimed at deciphering the basic web of genes that regulates cell reprogramming.

Here, we report a robust protocol for the isolation of large populations of highly viable and dividing protoplasts from in vitro–grown *Arabidopsis* plantlets. We established a liquid medium that supports a high rate of protoplast division (up to 50% of the protoplasts). This protocol allowed us to characterize the changes in the transcript profile during the early steps of dedifferentiation and reentry into the cell division process (i.e., from plantlets to 1-week-old PdC colonies). We present a spreadsheet that can be used for gene filtering of our large data set, enabling cross-comparisons with other studies. The protoplasts underwent rapid dedifferentiation and major changes in organelle metabolism, followed by reinitiation and reorientation of protein synthesis, striking changes in the expression of chromatin-associated genes, and reinitiation of cell division with cell wall rebuilding. Comparisons between PdCs and cells of a well-established cell suspension revealed epigenetic differences that suggest that PdCs are more closely related to plant tissues than to cells in suspension. Finally, our study identified an array of molecular factors that function in the early steps of reprogramming. By testing the functional roles of two of these factors, we show that the *ALF4* plant-specific factor is crucial for protoplast division. Thus, our data will serve as a valuable source of candidate genes for further investigations of plant cell plasticity and totipotency.

RESULTS

From Efficient Protoplast Culture in Liquid Medium to Plantlet Regeneration

A stable source of axenic plant material devoid of stresses (light, heat, and drought) is crucial for successful cell culture in liquid medium over extended periods of time. Therefore, we first optimized the in vitro culture conditions (i.e., climate, vessels, and media) for the production of *Arabidopsis* plantlets suitable for protoplast and plant regeneration. Our best results were obtained when plantlets were cultured in a Green Box container on germination medium (GM) (see Supplemental Table 1 online), placed in a growth chamber with 75% controlled relative humidity, short-day conditions, and a constant temperature of 20°C. For optimal yields of viable and dividing protoplasts, plantlets were collected 18 to 21 d after sowing. This narrow developmental window probably depended on complex environmental factors that influence the osmotic potential of seedlings, such as the progressive drying of the culture medium, as well as on developmental factors. We next established maceration conditions that allowed the treated cells to adapt progressively to the osmotic pressure of the maceration Gly Glc medium (MGG) (see Supplemental Table 1 online) and resulted in a moderate level of plasmolysis. Cell walls were slowly degraded by overnight exposure to low levels of cellulolytic enzymes. Under the conditions used here, only the aerial parts of seedlings were efficiently digested. Routinely, $\sim 3 \times 10^6$ protoplasts were released per gram of seedlings. More than 90% were viable, based on a fluorescein diacetate assay (Widholm, 1972) (Figures 1A and 1B).

To optimize the culture medium for high plating efficiency, we systematically estimated the influence of all of the components in the medium, as well as the environmental conditions, based on our previous successful in vitro cultures of protoplasts from various species, particularly hybrid poplars (*Populus tremula* × *Populus alba*) (Chupeau et al., 1993). Using this empirical approach, we established that 2,4-D is the least toxic synthetic auxin in our experimental setup, that thidiazuron (TZ) is the only cytokinin that permits the development of healthy protoplasts, and that the combined use of 2,4-D and TZ results in the highest division rates. We also established that low levels of ammonium and nitrate are essential for high division rates of *Arabidopsis* protoplasts in liquid culture. A low level of microelements (Heller, 1953) was added to the liquid protoplast culture to increase the division rate. The addition of folic acid to the formulation of vitamins (Morel and Wetmore, 1951) promoted *Arabidopsis* cell survival and division. Although a 9% (w/v) solution of Glc permitted cell division, a mixture of Glc (4% w/v) and mannitol (6% w/v) in the initial protoplast induction medium (PIM) was more effective at promoting division (see Supplemental Table 1 online).

Using our established PIM, 30 to 50% of the initially plated protoplasts plated at 8×10^4 protoplasts/mL routinely underwent cell division. The first division occurred 3 d after plating for a small population of nonchlorophyllous cells, mainly composed of protoplasts derived from companion cells of the phloem (the less differentiated cells in leaves; Buchanan-Wollaston et al., 2005). Other cell types first divided between 3 and 6 d after plating (Figure 1C). Considering the large range of cell type diversity in the isolated protoplasts, we assumed that such a plating efficiency was a good indication that the overall process, including the preparation and formulation of the media, was well adapted for *Arabidopsis* protoplast survival and division. During the first week of culture, PdCs progressively formed microcolonies (Figure 1C).

If left in the 2,4-D–containing PIM medium, *Arabidopsis* colonies became necrotic. Since a low level of auxin is known to favor the growth of cell colonies (Caboche, 1980), the necrotic response that we observed might be due to an excess of 2,4-D or to the absence of its conjugation by indole-3-acetic acid–amido

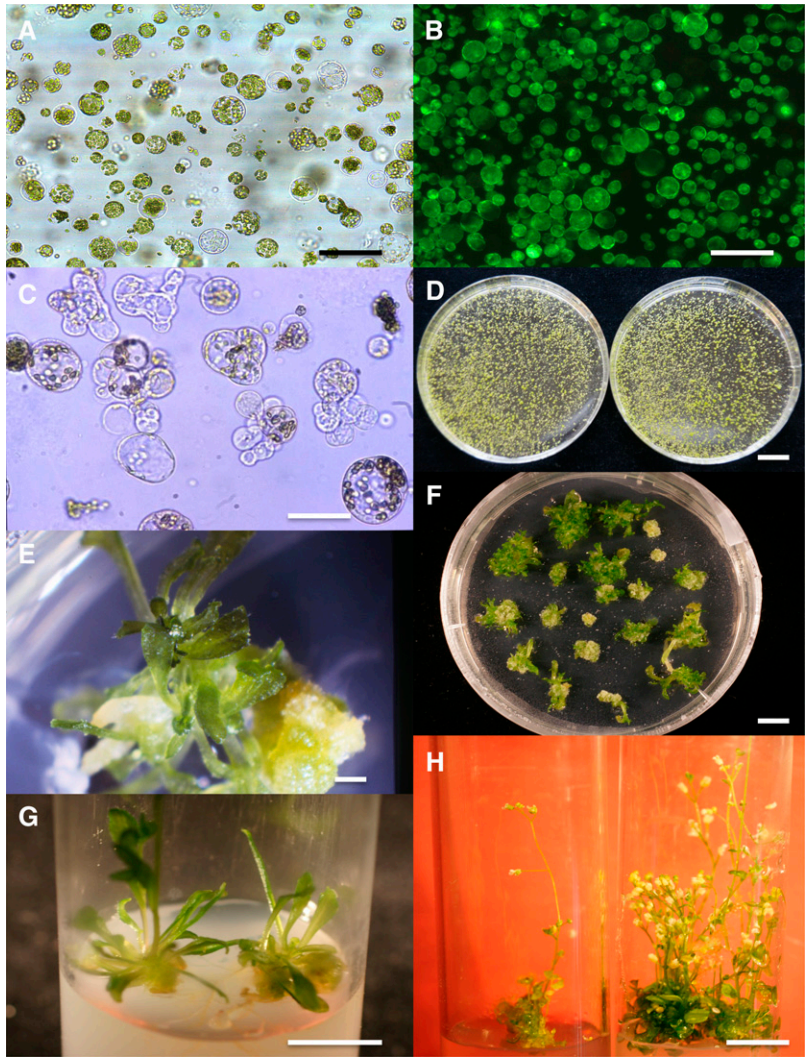

Figure 1. Regeneration of Plantlets from *Arabidopsis* Protoplasts.

(A) Different cell types of freshly isolated Col-0 protoplasts in maceration medium. Bar = 100 μm.
(B) Viable protoplasts (Col-0) fluoresce in fluorescein diacetate under UV light. Bar = 100 μm.
(C) Representative example of small cell colonies (Col-0) formed in a liquid culture dish after 6 d in culture. Approximately 25% of cells were dead, 25% survived, but were nondividing, and 50% had divided. Bar = 50 μm.
(D) Small cell colonies (Col-0) in liquid culture, 1 month after the second dilution in 10-cm dishes (two replicates). Bar = 1 cm.
(E) A rare example of a Col-0 colony differentiating buds on gelified SIM. Bar = 1 mm.
(F) Regenerating Ws colonies 20 d after transplantation onto gelified SIM. Bar = 0.5 cm.
(G) Development of Ws buds 1 week after transplantation onto rooting medium in culture tubes. Bar = 1 cm.
(H) Numerous flowering stems after 3 weeks of culture on rooting medium. Bar = 1 cm.

synthases (GH3). Thus, at day 11, we diluted the medium twofold with colony induction medium 1, which lacks auxin (see Supplemental Table 1 online) to decrease the auxin concentration and thus improve the viability of colonies and promote regeneration. One month later, we diluted the PdC suspension with medium enriched in nitrogen and containing TZ, but no auxin (2 mL suspension in 8 mL colony induction medium 2; see Supplemental Table 1 online), to ensure further growth of the microcalli (Figure 1D). Since we never observed bud formation in liquid medium, regardless of the phytohormones present, we transplanted colonies onto semi-solid medium for the subsequent regeneration steps. By comparing the effects of various cytokinins at different concentrations, we found that meta-topolin [6-(3-hydroxybenzylamino) purine] (Aremu et al., 2012) was the most effective at promoting regeneration. We therefore included this compound in the shoot induction medium (SIM; see Supplemental Table 1 online). Approximately 3% of Columbia-0 (Col-0) microcalli formed buds on the SIM medium, whereas

up to 90% of Wassilewskija (Ws) calli differentiated buds (Figures 1E and 1F). After the buds were transplanted onto plant development medium (see Supplemental Table 1 online), young plantlets developed for both accessions, generating inflorescences (Figures 1F to 1H). Therefore, the Ws accession was better able to regenerate from protoplasts than was the Col-0 accession, confirming previous results obtained with root explants and leaf calli (Candela and Velazquez, 2001; Zhao et al., 2013). Thus, Ws and Col-0 protoplasts derived from various cell types of the aerial parts of plantlets were able to reenter the cell cycle and, ultimately, regenerate plants.

Experimental Transcript Profiling Scheme

To investigate the early steps of regeneration (i.e., reentry into the cell cycle from differentiated cells), we compared the transcript profiles of 3-week-old plantlets grown in soil (Pls) or in vitro (Pliv), of freshly isolated protoplasts (P0), and of PdCs during the first week of culture (after 24, 48, 96, and 168 h of culture; hitherto referred to as P24, P48, P96, and P168). To assess the effect of prolonged in vitro culture, we also examined the transcript profile of well-established *Arabidopsis* cell suspensions (C) (Figure 2). We used Complete *Arabidopsis* Transcriptome MicroArrays (CATMA v2.1) for this study (Crowe et al., 2003; Hilson et al., 2004). Because Col-0 and Ws protoplasts underwent similar changes during the first week of culture (i.e., they both reentered the cell cycle and formed microcolonies) and because CATMA microarrays are based on the Col-0 genome, we performed our transcript analyses using Col-0 material. Massive (8984) transcriptomic changes took place during the first week of protoplast culture, corresponding to 5276 different genes being differentially expressed (Table 1). There was a remarkable balance between the number of genes that were up- and downregulated in each comparison, except that there was a bias toward downregulation in the Pliv/Pls comparison (Table 1).

These data are presented in a searchable format to facilitate analysis and sorting of profiles and information (see Supplemental Data Set 1 online). Supplemental Data Set 1 online includes a user-friendly spreadsheet (gene selector) that was designed with advanced Excel functions to extract expression profiles using lists of genes sorted by AGI annotations. The expression of a small subset of genes was monitored by quantitative RT-PCR to verify our CATMA data (see Supplemental Table 2 online).

Transcriptome Comparison between Plants Grown in Soil and in Vitro

To identify changes induced by in vitro culture itself, we used the same growth conditions (i.e., photoperiod, light intensity, and nutrition) for plantlets grown in soil and in vitro. As expected, few differences were detected in the transcriptomes of plants grown in vitro and those grown in soil (Pliv/Pls; Table 1). The bias between the number of up- and downregulated genes in this comparison prompted us to analyze the Gene Ontology (GO) annotations of the 325 downregulated genes using the Bio-Array Resource for Plant Functional Genomics (BAR) classification superviewer program. The analysis revealed a strong enrichment for genes involved in electron transport or energy pathways and in the response to abiotic or biotic stimuli (3.27 and 3.23 normed frequencies, respectively) and in genes encoding plastid components (4.23 normed frequency). The Pliv/Pls transcript profile comparison reflected adaptations of the photosynthetic apparatus, cell walls, and chromatin composition in plantlets cultured in vitro. Among the downregulated genes, we identified genes encoding two *CELLULOSE SYNTHASE* genes (*CESA1* and *CESA3*), one chitinase (AT2G43620), the fasciclin-like protein FLA9, a pectinacetylesterase (AT2G46930), and the HTR12 centromeric histone. Among the 30 upregulated genes, we noticed an enrichment in genes involved in other biological processes and in the response to stress (3.52 and 2.99 normed BAR frequencies, respectively) and in several transcription regulators (i.e., *LATE EMBRYOGENESIS ABUNDANT3* and *MULTIPROTEIN BRIDGING FACTOR1C*), which may be interesting candidates for genes involved in the adaptation to in vitro culture

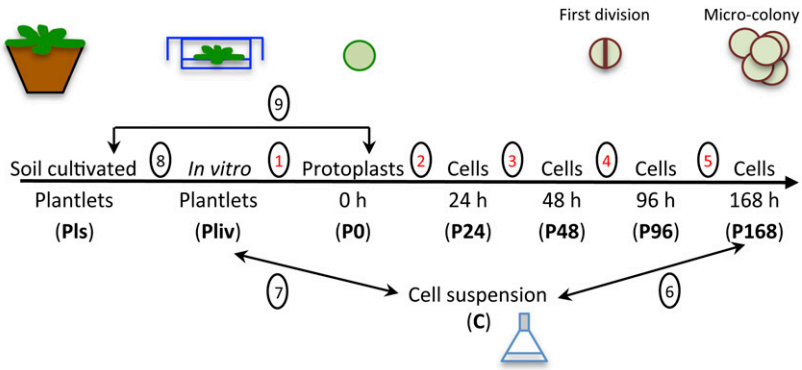

Figure 2. Transcript Profiling Experimental Design.

The transcript profiles of eight different samples were compared, and the first five comparisons used in the hierarchical clustering analysis are numbered in red.

Table 1. The Nine Transcript Profile Comparisons and the Number of DEGs for Each Comparison

Transcriptomes		All Deregulated Genes	Genes Upregulated	Genes Downregulated
1	P0/Pliv	3507	1728	1779
2	P24/P0	2635	1284	1351
3	P48/P24	538	308	230
4	P96/P48	1209	648	561
5	P168/P96	1095	541	554
6	C/P168	2796	1378	1418
7	C/Pliv	4187	2182	2005
8	Pliv/Pls	355	30	325
9	P0/Pls	4661	2273	2388

conditions (see Supplemental Data Set 1 online, column AM). Thus, our data highlighted a small set of candidate genes likely to be involved in in vitro adaptation.

Eight Gene Clusters Reflect the Transition from in Vitro–Grown Plantlets to 1-Week-Old PdCs

Of the five successive transcriptome variations present from in vitro–grown plantlets to and P168, we identified 8984 variations in transcription, concerning 5276 differentially expressed genes (DEGs; Table 1, Figure 3A), with complex profiles (this set of 5276 DEGs was annotated as DE5). The largest number of DEGs was identified in fresh protoplasts (P0/Pliv: 3507) and at P24 (P24/P0: 2635), suggesting that most dedifferentiation and reprogramming events occur within the first day of culture. Surprisingly, the first five sets of DEGs shared a common set of 37 genes that was enriched in response to stress, suggesting that a permanent, but partial, wounding state is maintained throughout the process (Figure 3B). In parallel with the activation of the basal stress response, dramatic global changes occurred in the expression of genes involved in various processes, which we detected in an analysis of enriched GO terms using the agriGO toolkit. For instance, DE5 genes involved in lipid transfer and in the synthesis of the photosynthesis apparatus were downregulated in freshly isolated protoplasts, those involved in nuclear and RNA processes were reactivated from 24 h (P24), and those that activate cell division were mostly upregulated at 96 h (P96; Figure 3C).

Clustering analysis of the 5276 DEGs using the Multiexperiment Viewer tool revealed eight main clusters (C1-8; Figure 4A; see Supplemental Figure 1 online) comprising 3873 genes (73%). The entire list of genes in each cluster is presented in Supplemental Data Set 1 online (columns AR-AY), and a diagram representing the changes in transcript levels over time is shown in Figure 4B. The expression of most genes (C1-6) changed from 0 to 24 h, suggesting that the major events underlying changes in cell fate occur in the 0 to 24 h developmental window. Interestingly, at least 592 of the genes that were upregulated in freshly isolated protoplasts remained upregulated throughout the entire culture period (C1; Figure 4B).

To better characterize the clusters, we performed GO analysis (Table 2; see Supplemental Table 3 online). This approach highlighted functional specificities for each cluster according to the main GOs present in the clusters and a progression during protoplast culture from stress response to reprogramming processes. The C1 and C2 clusters mainly contained genes involved in stress responses, whose expression seems to be required during the week of culture. However, whereas C1 also contained upregulated genes related to electron transport and the energy pathway, C2 included downregulated genes involved in cell organization, photosynthesis, and biogenesis. In the C3 cluster, various genes involved in DNA and RNA metabolism pathways were upregulated, as were genes related to electron transport and the energy pathway, suggesting the reorientation of cellular fate. In parallel, genes associated with transport and communication were downregulated (C4). Interestingly, a set of genes associated with stress responses were transiently up- and downregulated (C5), suggesting that they are related to protoplasting reactions. The C7 and C8 clusters contained genes required for DNA or RNA metabolism, signal transduction, or developmental processes. Interestingly, the postembryonic development GO annotation (GO:0009791) was significantly represented in clusters C2, C3, and C8, suggesting that three specific and distinct sets of genes involved in this process were successively downregulated at 0 h and then progressively activated at 24 h and 96 h.

The C5 and C6 clusters presented a rapid reversal of expression profiles between protoplasts and P24 and contained the largest set of DEGs (1345). In a study of the *Arabidopsis* apical meristem, 300 genes were identified as responding to protoplasting treatment (Yadav et al., 2009). This discrepancy may be due to differences in maceration times and starting material in the previous study and ours, which identified a larger set of genes corresponding to the C5 and C6 clusters. Furthermore, the C5 and C6 clusters together contained fewer than the 6323 genes identified as being involved in natural leaf senescence (Breeze et al., 2011). This observation indicates that the dedifferentiation process in protoplasts differs from that in senescence. Overall, cross-analysis of stress genes (GO:0006950) and DEGs in senescence (Breeze et al., 2011) revealed that the 5276 DE5 genes during the whole process had 2358 genes in common with senescence and 1313 in common with the stress response (see Supplemental Figure 2 online). The largest number of genes related to the stress response were found in cluster C5, partially confirming that C5 is associated with mostly reversible stress reactions that occur during protoplasting.

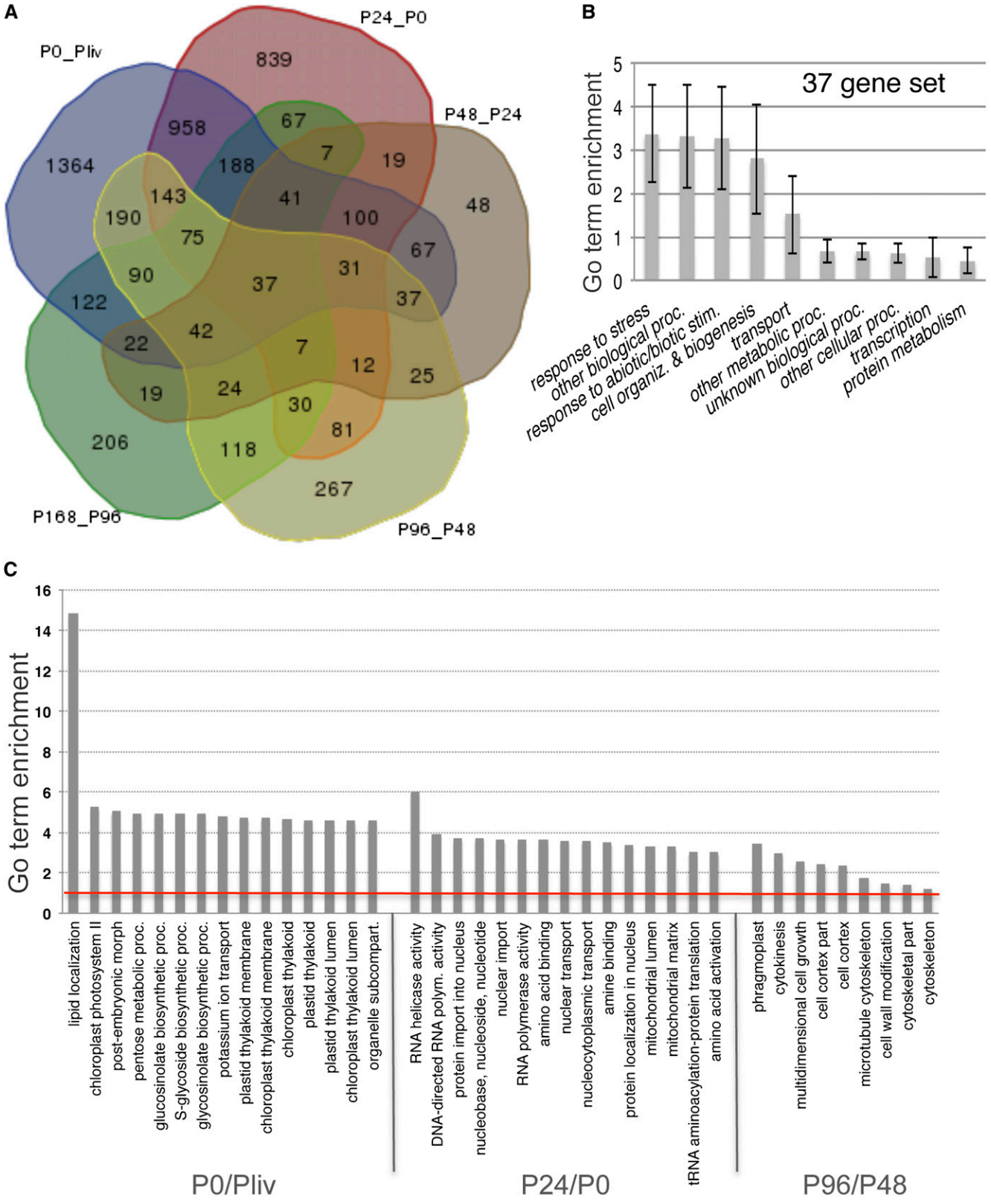

Figure 3. Genes Differentially Expressed during the First Week of Culture.

(A) Venn diagram representing the five first transcriptome comparisons (i.e., from in vitro plantlets to P168).

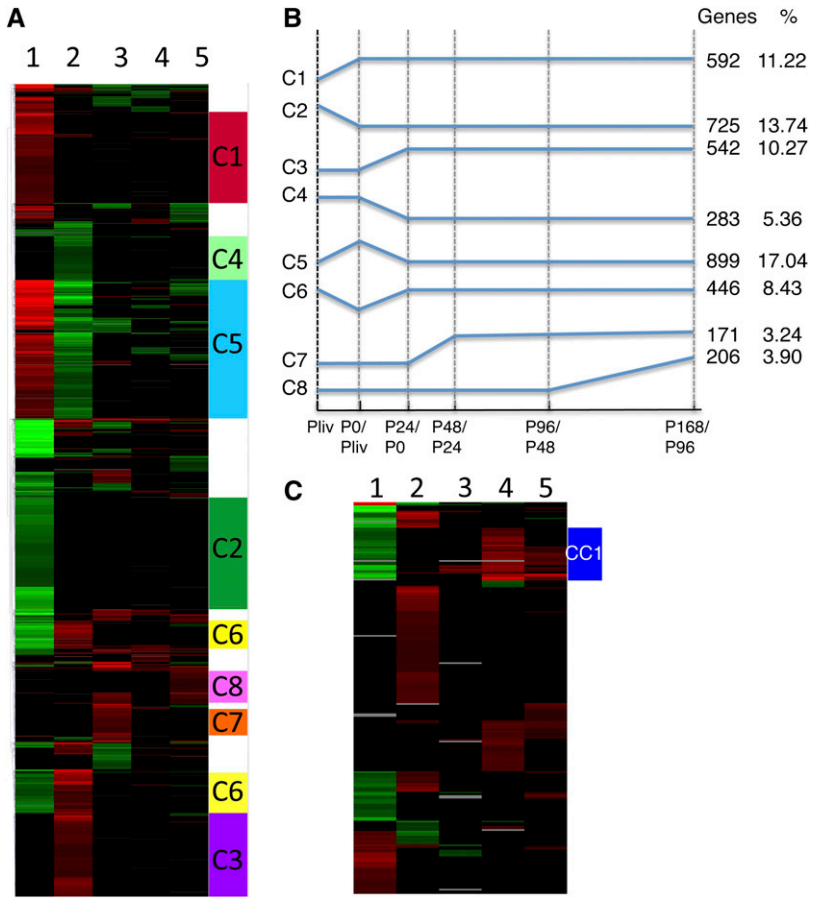

Figure 4. Clustering Analysis of DEGs during the Transition from in Vitro–Grown Plantlets to 1-Week-Old PdCs.

(A) Hierarchical clustering using Multiexperiment Viewer of the transcript profiles from in vitro–grown *Arabidopsis* plantlets to P168. The 3864 genes (73% of DEGs in the DE5 set) were distributed into eight main clusters (see Supplemental Data Set 1 online).
(B) Schematic representation of the eight clusters. The number of genes in each cluster and the percentage of DEGs (out of 5276 total) represented in each cluster are given.
(C) Cell cycle and cell division DEGs in *Arabidopsis* protoplasts during culture. Hierarchical clustering highlighting a cell cycle–specific cluster (CC1, in blue). The genes used are listed in Supplemental Data Set 1 online.

A comparison of our data set with transcriptome data of *Arabidopsis* protoplasts freshly isolated from Landsberg *erecta* plantlets (Damri et al., 2009; Grafi et al., 2011) or from meristematic tissues (Yadav et al., 2009) revealed a set of common deregulated genes that might be markers of the protoplasting process. Among the 576 transcription factors (TFs) identified by Grafi et al. (2011) and Damri et al. (2009), 179 TFs were deregulated in our experiments, and 90 out of the 261 genes identified as being deregulated upon exposure of meristematic tissues to protoplasting conditions (Yadav et al., 2009) were also present in our list of DE5 genes (see Supplemental Table 4, Supplemental Figure 3, and Supplemental References 1 online). Six TFs and two heat shock factors were found to be deregulated in all three studies (see Supplemental Table 4 online). A few DE5 genes identified in our study were also among the list of genes associated with meristematic activities (Yadav et al., 2009), and most of these were downregulated (see Supplemental Table 5 online).

Figure 3. (continued).

(B) GO term enrichment analysis of the set of 37 genes present in all of the first five conditions using the BAR program. The bootstrap SD was calculated using the BAR SuperViewer tool (http://bar.utoronto.ca/ntools/cgi-bin/ntools_classification_superviewer.cgi).
(C) GO term enrichment analysis of P0/Pliv, P24/P0, and P96/P48 using the agriGO tool.
The top 15 GO terms from the analysis are presented for the first two conditions (PO/Pliv and P24/P0), and GO terms with a ratio of >1 are shown for the third condition (P96/P48). P value < 0.001.

Table 2. GO Analysis of the Eight Main Clusters of DEGs

Cluster	GO Biological Process (BAR Analysis)	GO Molecular Function	GO Cellular Comp.	GO Biological Process (AgriGO Analysis)		FDR
C1	Electron transport or energy pathways	Kinase activity	Cytosol	GO:0050896	Response to stimulus	4.4e-06
	Response to abiotic or biotic stimulus	Nucleotide binding	ER	GO:0042221	Response to chemical stimulus	4.4e-06
				GO:0044248	Cellular catabolic process	9.4e-05
				GO:0044265	Cellular macromolecule catabolic proc.	0.0006
C2	Electron transport or energy pathways	Other enzyme activity	Plastid	GO:0010876	Lipid localization	0.00031
	Cell organization and biogenesis	Other molecular functions	Cell wall	GO:0009791	Postembryonic development	0.00035
				GO:0015979	Photosynthesis	0.007
				GO:0016144	*S*-glycoside biosynthetic process	0.027
C3	DNA or RNA metabolism	Structural molecule activity	Cytosol	GO:0006396	RNA processing	2.7e-07
	Electron transport or energy pathways	Nucleotide binding	Ribosome	GO:0016070	RNA metabolic process	3.4e-07
				GO:0006139	Nucleobase, nucleoside, nucleotide, and nucleic acid metabolic proc.	3.4e-07
				GO:0009791	Postembryonic development	6.1e-07
C4	Transport	Receptor binding or activity	ER	NS		
	Other biological processes	Transporter activity	Plastid	NS		
C5	Response to stress	Receptor binding or activity	Cytosol	GO:0006950	Response to stress	7.2e-22
	Response to abiotic or biotic stimulus	Other enzyme activity	Other cytoplasmic comp.	GO:0050896	Response to stimulus	1.0e-17
				GO:0042221	Response to chemical stimulus	1.0e-17
				GO:0010033	Response to organic substance	1.5e-12
C6	Protein metabolism	Structural molecule activity	Ribosome	GO:0006412	Translation	3.2e-62
	Electron transport or energy pathways	DNA or RNA binding	Cytosol	GO:0044267	Cellular protein metabolic proc.	7.3e-35
				GO:0019538	Protein metabolic process	4.7e-30
				GO:0009058	Biosynthetic process	8.4e-30
C7	DNA or RNA metabolism	Other molecular functions	Golgi apparatus	NS		
	Signal transduction	Kinase activity	Cytosol	NS		
C8	Other biological processes	Kinase activity	Cell wall			
	Developmental processes	Hydrolase activity	Plasma membrane	GO:0009791	Postembryonic development	0.029

ER, endoplasmic reticulum; FDR, false discovery rate; NS, no significant enrichment in a GO could be identified.

Previously, the transcriptomes of *Physcomitrella patens* protoplasts were established at 0, 24, 48, and 72 h after isolation (Xiao et al., 2012). Among the DE5 set of genes identified in our study, 73 and 39 genes were similarly deregulated in moss at the P0/P24 and P24/P48 transitions, respectively. The small number of genes in common may result from the evolutionary distance between the two species and from differences in culture conditions. For instance, the moss protoplasts were cultured in the absence of exogenously added growth substance and under different photoperiod conditions. Most of these DEGs encode proteins involved in RNA metabolism, protein translation (ribosomal protein genes), and in the synthesis of the photosynthesis apparatus. *Arabidopsis* transcription regulators (e.g., *ERF1*, *BZIP63*, *TIFY10B*, and *NFXL1*) and their moss homologs that were deregulated in both of these species (see Supplemental Table 6 online) appeared mostly in C5. Since genes present in C5 were transiently deregulated, these DEGs that are common to *Arabidopsis* and moss represent protoplast markers of cell reprogramming that are independent of protoplasting conditions and species.

Responses of Freshly Isolated Protoplasts

In freshly isolated protoplasts, we detected changes in metabolism that resembled those linked to senescence. For instance, antioxidant pathways were stimulated and various organic metabolites and macromolecules were remobilized through the action of

hydrolases (e.g., lipases, proteases, and cellulolytic enzymes) and the proteasome pathway. However, only 2358 of the 6326 genes deregulated during natural senescence (Breeze et al., 2011) were also among the 5276 DE5 genes (see Supplemental Figure 2 online). In protoplasts, this remobilization pathway is activated dramatically faster than in a senescing leaf, where the process lasts for over 20 d (Breeze et al., 2011). However, PdCs could continue to dedifferentiate while already engaged in division, as ~50% of genes deregulated at each time point were also deregulated during senescence. Noticeably, only 10% of the genes that were stably activated from 24 h (C3) were involved in senescence, a first indication that most C3 genes may have specific roles in reprogramming.

The main difference between senescence and dedifferentiation was the rapidity with which genes involved in photosynthesis were downregulated in protoplasts. Whereas the downregulation of these genes occurred mostly within 24 h in protoplasts, it occurred later in the senescence process (from day 31 after germination; Breeze et al., 2011). A strong response to dehydration was observed in the freshly isolated protoplasts, as exemplified by the net activation of *EARLY RESPONSIVE TO DEHYDRATION1*, which promotes protein hydrolysis in chloroplasts (Nakashima et al., 1997). The chlorophyll synthase *CHLG* and most of the genes encoding chlorophyll *a/b* binding proteins and proteins of the photosystems were also downregulated during protoplast isolation. The *GLK2* TF, which coordinates photosynthesis; *HEMA1*, the glutamyl-tRNA reductase gene involved in tetrapyrrole synthesis; and genes that regulate the stability of chloroplast-encoded transcripts (*HCF152* and *173*) were downregulated in protoplasts (see Supplemental Data Set 1 online). However, chloroplast degradation was not complete in protoplasts, and some of their essential cellular roles were preserved.

Although six senescence-associated genes (*SAG1*, *3*, *13*, *20*, *24*, and *29*) were strongly upregulated in P0, *SAG12*, which encodes a Cys protease active in chloroplast degradation during late leaf senescence, was not activated in protoplasts. The upregulation of *SPERMINE SYNTHASE* in P0 could be related to the response to oxidative stress, as the homolog in mouse (*Mus musculus*) was found to be involved in this process (Eisenberg et al., 2009).

Concurrent with metabolic shifts occurring in the protoplasts, the cells exhibited a hypoxic stress response, as indicated by the activation of key genes involved in glycolysis (e.g., phosphofructokinases [*PFK3* and *PFK7*] and pyruvate kinase). The upregulation of a hemoglobin gene (*GLB3*) and of genes encoding alcohol dehydrogenases (*ADH* and *ATA1*) was also indicative of hypoxia, which represented an additional stress to protoplasts. Furthermore, the stable upregulation of the hypoxia responsive gene (AT5G27760) revealed that hypoxia persisted throughout culture in Petri dishes. Hypoxic conditions probably developed because the cultures were grown without agitation, and protoplasts tend to sink despite the small volume of liquid medium used in our study (depth of medium ~1.5 mm of liquid in a Petri dish). Similarly, out of the 1728 genes activated in P0 (Table 1), 592 genes (C1; Figure 4B) were permanently activated during the first week of culture, among which 168 were stress-related genes. These observations confirmed that PdCs maintain a permanent but partial wounding state.

Interestingly, two phytosulfokine genes (*PSK2* and *PSK4*) encoding intercellular signal peptides involved in cell proliferation and a receptor kinase gene (*PSKR1*) (Matsubayashi et al., 2002) were upregulated in P0 (see Supplemental Data Set 1 online). At the onset of culture, the composition of the medium changed rapidly due to exchanges between cells and the medium and the transmission of signals, such as phytosulfokines, between cells. Thus, an analysis of the extracellular proteins and receptors involved in protoplast preparation and culture may shed light on the conditioning effect that cells have on the medium, which results in a certain starting cell density (8×10^4 per mL in our case) having optimal rates of plant cell division in vitro.

Therefore, even in our moderate maceration conditions, the response to injury was part of a fast and specific dedifferentiation process that yielded a fairly homogeneous population of cells by coordinating various regulatory pathways that led to cell division competence. The homogeneous and high rate of protoplast division in response to auxin and cytokinin confirmed that most protoplasts reached a similar cell state.

Protein Biosynthesis Reorientation during Protoplast Culture

As key components of the protein biosynthesis machinery, ribosomes play crucial roles in regulating growth. The expression of ribosomal protein genes (*RP*s) is tightly developmentally and environmentally regulated (Chantha et al., 2007). Using an *RP* gene list (Barakat et al., 2001), we observed major changes in the transcript abundance of 130 genes encoding RPs, corresponding to ~60% of the cytoplasmic *RP* genes present in the CATMA microarray (total 220 genes on the microarray; Table 3; see Supplemental Data Set 1 online, columns BQ and BR). Most *RP* DEGs clustered into C6 (Table 3). Among the *RP* genes upregulated at 24 h, a small fraction was downregulated later during the protoplast culture. In total, 26 out of the 32 RP genes of the small subunit family (RPS) present in the *Arabidopsis* genome were affected, whereas only 25 of the 48 RP large subunit (RPL) family members present were affected, suggesting that ribosome composition is predominantly regulated by modulating RPS composition. Interestingly, two homologs of the *Drosophila melanogaster NOTCHLESS* gene involved in cell fate decision and developmental processes through the Notch pathway and ribosomal biogenesis were also upregulated from 24 h (*NLE* and *NLE1*). *NOTCHLESS* plant homologs have been shown to regulate cell growth and proliferation (Chantha et al., 2006). Another gene that regulates ribosomal biogenesis (*RRS1*) also clustered in C3. *NUCLEOLIN* genes (*NUC-L1* and *NUC-L2*) involved in pre-rRNA processing (Pontvianne et al., 2010) were also upregulated at 24 h. Therefore, protein biosynthesis resumed rapidly during protoplast culture by the direct modulation of *RP* transcription and of several nonribosomal regulatory factors. These data suggest that four combinatorial sets of *RP*s (C2, C3, C5, and C6; Table 3) are important throughout the process and that the ribosomal equipment needs to be precisely regulated during reentry into the cell cycle. Further investigation of the expression of ribosome transacting factors, such as *SWA1* (Shi et al., 2005) (absent from the CATMA microarray), that

Table 3. Distribution of Ribosomal Protein Genes in the Eight Clusters of DEGs Identified in *Arabidopsis* Protoplasts

Cluster	RP Number	1	2	3	4	5	AGI Identifier/Name
C1	0	Up	nc	nc	nc	nc	
C2	6	Dn	nc	nc	nc	nc	RPL22A, RPP2C, RPS15aE, RPS15F, RPS17C, RPS19B
C3	6	nc	Up	nc	nc	nc	RPL10B, RPL39B, RPL7D, RPL9D, RPP0C, RPSaB
C4	0	nc	Dn	nc	nc	nc	
C5	2	Up	Dn	nc	nc	nc	RPL18aA, RPL10C (SAG24)
C6	101	Dn	Up	nc	nc	nc	RPS18A (PFL1), (RPS13A (PFL2),(RPL24 (STV1), L10aP (PIGGYBACK1), RP1 (EMB2207), AT3G04400 (EMB2171), AT3G48930 (EMB1080), RPS6B (EMB3010), AT1G58380 (XW6) (see Supplemental Table 1 online, columns AW and BQ, for a complete list)
C7	0	nc	nc	Up	Up	nc	
C8	0	nc	nc	nc	nc	Up	
Others	15	nc	nc	nc	nc	nc	
Total DEGs	130	nc	nc	nc	nc	nc	

Up, upregulation; Dn, downregulation; PFL, pointed first leaf; RPL, RP large subunit; RPS, RP small subunit; SAG, senescence-associated gene; STV, short valve; EMB, embryo defective; nc, no change in expression.

regulate division would facilitate the characterization of RP regulation in our system.

Regulation of protein translation also modulates the protein content of a cell during various adaptive responses, with the initiation of translation being the main target of such regulatory mechanisms. In our data set, four translation initiation factor genes were upregulated (C1 and C3; see Supplemental Data Set 1 online). Furthermore, *RACK1*A (for *Receptor for Activated C Protein Kinase1*), a component of the plant 40S ribosome subunit that regulates translation (Chang et al., 2002; Giavalisco et al., 2005; Guo et al., 2011), clustered in C6, and accordingly was also upregulated at 24 h. Another means of regulating protein composition during protoplast culture is protein degradation. Indeed, genes encoding 26S/ubiquitin were sequentially activated and repressed during the transition from plants to protoplasts and then between different time points of the protoplast culture. These drastic events affecting protein metabolism represent indicators of dedifferentiation and reprogramming during the first 24 h of culture.

Progression into the Cell Cycle

Since auxin and cytokinin are key regulators of plant cell division, we investigated the expression of genes involved in their biosynthesis and regulation. In the cytokinin regulatory pathway, only a few genes were deregulated: *IPT8*, which is involved in cytokinin synthesis, three response regulators (*ARR4*, *ARR6*, and *ARR7*), and two cytokinin response factors (*CFR1* and *3*) were activated at 24 h. *ARR16* was upregulated from 96 h onwards.

The expression profiles of auxin-related genes were more complex. In protoplasts, the auxin biosynthesis pathway was activated, as suggested by the upregulation of Trp synthases, nitrilases, and specialized cytochrome P450 genes. This early activation resulted from the wounding response of protoplasts, since most of these were deactivated later in the process (see Supplemental Table 7 online). In addition to the early indole-3-acetic acid burst, 2,4-D (i.e., synthetic auxin) in the culture medium may regulate the auxin biosynthesis pathway. Genes encoding conjugating enzymes (*GH3-2* and *GH3-3*) were also activated early in the process, and their expression was maintained throughout the culture period. The auxin signaling pathway was also modified, with auxin efflux carrier genes being deregulated. Two main subsets of efflux carriers could be distinguished based on their expression profiles, suggesting different functions: One class (containing *PBP1*) was upregulated at P0 and downregulated later, the other (containing *PIN1*, *PIN6*, and *MEE21*) was upregulated after P0, at different time points. Interestingly, from 24 h onwards, two auxin signaling F-box (*AFB*) genes encoding auxin receptors, *AFB2* and *AFB5*, were upregulated.

Noticeably, *IAA14*, *ARF7*, and *ARF19*, which are involved in the auxin pathway and are activated during lateral root initiation (Vanneste et al., 2005), were not deregulated, whereas *IAA7*, *IAA8*, *IAA9*, *IAA20*, *IAA29*, *ARF4*, *ARF5*, and *ARF6* seemed to be involved in the early steps of protoplast-based regeneration (see Supplemental Table 7 online). The array of genes deregulated in protoplasts was also different from that deregulated during leaf callus initiation (He et al., 2012). The calossin-like *BIG* gene, which participates in the vesicular targeting of auxin transporters and is required for pericycle cell activation in lateral root primordia (Gil et al., 2001; López-Bucio et al., 2005), was upregulated, as were other genes known to be associated with the pericycle (Parizot et al., 2010) (see Supplemental Table 7 online). These data suggest that a specific auxin-mediated pathway is activated during protoplast culture.

We established a list of 384 genes related to the cell division cycle and cytokinesis based on GO annotations (GO:0007049, GO:0051301, GO:0000910, and GO:0000280) and on reports in the literature (Gutierrez, 2009) (see Supplemental Data Set 1 online, columns BE-BJ tagged as cell cycle). Among them, 373 genes were deregulated in the DE5 set, and a specific cell cycle cluster (CC1) of 31 genes expressed in plantlets was downregulated

in the transition to protoplasts and then reactivated at 96 h. The deregulation of genes in CC1 suggests a reversion to a pluricellular organization and cell division control in the microcolonies (Figure 4C).

During the first week of culture, a wave of cell cycle–related gene activation was observed, concomitant with resumption of cell division, which peaked at 96 h and was followed by the formation of microcolonies (see Supplemental Figure 4 online). Downregulation of cell cycle–related genes was largely limited to the protoplasting step (see Supplemental Figure 4 online). Our data highlight a specific role for two cyclin-dependent kinase inhibitor genes (*KPR1* and *KRP6*) in cell cycle arrest during protoplast isolation. At P24, *CUL1* and *AXR1*, which regulate protein degradation activity, may promote cell cycle progression by degrading KRPs. Furthermore, the activation of *CYCH1-1*, which has a role in cyclin-dependent kinase–mediated activation, and of *REPLICATION PROTEIN A1* seems to mark entry into the S phase during early protoplast development.

Between 48 and 96 h, *PCNA1* and *PCNA2*, two key factors of the DNA replication machinery, were upregulated, along with DNA replicating factors (*MCM3*, *4*, and *10*). At 96 h, *CYCA1-1* and *CYCA3-2*, which are specific to the G2 phase, were upregulated, along with *CYCB1;4* and *CDKB2;1* and two *AURORA* genes (*AUR1* and *AUR2*) (Demidov et al., 2005). These last four genes were not clustered because they were also upregulated at 168 h, thus confirming that a first round of mitosis occurred at around 96 h of culture for most PdCs. At 168 h, *CDKB2;1*, *CYCB1;4*, *CYCB2;2*, and *CYC3B*, which are also involved in the G2/M transition and mitosis (Dewitte and Murray, 2003), along with *TANGLED*, which plays a role in cytokinesis and phragmoplast guidance (Walker et al., 2007), were reactivated, marking active cell divisions and the formation of microcolonies. *POLTERGEIST* (*POL*), which acts downstream of the *CLAVATA* signaling pathway in meristem development and is required for stem cell maintenance, was also reactivated in the microcolony stage, which may suggest the onset of functional cellular organization and the formation of cellular mass. In roots, cell divisions are arrested by KRP2 and stimulated by auxin signals and specific cyclins (CYCD3;2, CYCA2;4, and CYCB2;5) (Vanneste et al., 2005). Thus, protoplast culture seems to require a different and specific set of cell cycle–related genes. The protoplast cell cycle progression gene module sequentially activates KRP1/KRP6/CDKC1, CYCH1, CYCA3;2, CYCA1/SIM/PCNA, and CYCB/CDKB2;1/POL. Until now, CDKCs were thought to regulate transcription without directly regulating the cell cycle (Cui et al., 2007). The activation of CDKC1 after 24 h of culture suggests that this protein has a specific role in reactivating protoplast division.

Cell Wall Reestablishment during the First Week of Culture

Cell wall reorganization is essential for protoplast survival and adaptation to the external medium. This complex process is regulated by numerous enzymes and relies on interactions with the cytoskeleton, which determines microfibril orientation (Szymanski and Cosgrove, 2009) and facilitates the extracellular delivery of polysaccharide precursors via Golgi-derived vesicle trafficking (Parsons et al., 2012). As the complete set of genes involved in the elaboration of the cell wall has not yet been established, we selected 285 genes involved in cell wall synthesis based on GO annotations (GO:0071554 and GO:0009664) and the literature (see Supplemental Data Set 1 online, columns BA to BD).

Briefly, clustering analysis of 217 cell wall–tagged genes, such as those encoding pectin lyases and plant invertases, revealed that 42% of the genes were excluded from the eight main clusters identified in this study and showed complex profiles (see Supplemental Data Set 1 online). Most of these genes (112 out of 217) were downregulated in fresh protoplasts and progressively reactivated during culture with kinetics specific for each gene. Two closely related *EXPANSIN* genes (Kende et al., 2004), *EXPAI* and *EXPA10*, were strongly upregulated from 24 h onwards, and six others were upregulated later during culture. This could indicate additional functions for this protein family besides roles in cell wall loosening and abscission (Sampedro and Cosgrove, 2005). A large group of cell wall–related genes was upregulated from 96 h of culture onwards, concomitant to the reorganization of the cytoskeleton and phragmoplast after the first round of PdC division. Consistent with this finding, *CSLC04* and *CSLC06*, two Golgi-located glucan synthases (Parsons et al., 2012), were activated from 96 h onwards.

Rather surprisingly, only two cellulose synthase genes, *CESA1* and *CESA3*, were upregulated early and late during the culture period. This suggests that cellulose synthesis was regulated at the posttranscriptional level in protoplasts. Alternatively, cellulose organization may be a continuous process. This possibility is supported by the almost immediate reappearance of microfibrils in freshly isolated and washed protoplasts (Kwon et al., 2005). Our profiling could provide additional data for deciphering this complex cell wall rebuilding process and the mechanisms that regulate it (Kwon et al., 2005; Yang et al., 2008).

Putative Roles of Organelles in the Reentry into the Cell Cycle

Many nuclear genes encoding proteins targeted to mitochondria and chloroplasts were deregulated in our study; thus, organelles appear to have an important role in the early changes in cell machinery and possibly also in the dedifferentiation process. Nuclear genes that regulate chloroplast division, which precedes cell division, were upregulated by as early as 24 h (i.e., *FtsZ*, a DNAJ gene, and *ARC6*, which encodes a factor promoting the plastid-dividing *FtsZ* ring). Surprisingly, though protoplasts were cultured in the dark, a small number of photosynthetic genes were also activated (i.e., four magnesium chelatase genes and two chlorophyll *a*/*b* binding genes). Pentatricopeptide repeat (PPR) proteins are involved in many aspects of RNA processing in organelles. Mutations in *PPR* genes generally have pronounced effects, and most are embryo lethal (Schmitz-Linneweber and Small, 2008). PPR proteins form one of the largest families in the *Arabidopsis* genome, with 450 members (Lurin et al., 2004; Fujii and Small, 2011). Twenty *PPR* genes were deregulated in our study, five of which were specifically activated in C3 and one of which was downregulated in Pliv/Pls.

WHIRLY2, encoding a DNA binding protein involved in gene regulation and essential for proper mitochondrial function (Maréchal et al., 2008), was activated from 24 h onwards. Posttranscriptional control is important for the proper regulation of mitochondrial gene expression, since mitochondrial genes are generally not regulated at the transcriptional level (Holec et al., 2006). The mitochondrial exoribonuclease, which belongs to the polynucleotide phosphorylase family (AT5G14580) and is involved in mRNA metabolism, was also strongly activated from 24 h. This gene product is vital, as downregulation of the corresponding gene causes unprocessed RNAs to accumulate (Perrin et al., 2004). The importance of organelle RNA metabolism in PdCs is reminiscent of the early events in mitochondrial biogenesis during germination (Law et al., 2012).

Interestingly, three prohibitin genes (*PROHIBITIN1*, *3*, and *6*) were activated from 24 h onwards. PROHIBITIN proteins play crucial stress protective roles in mitochondria, but also regulate cell proliferation (Merkwirth and Langer, 2009), and as such are needed for planarian regeneration (Reddien et al., 2005). Genes involved in metabolism were also specifically activated early in the process; for example, *GOGAT2*, a chloroplast gene essential for amino acid biosynthesis, and two genes encoding mitochondrial ATP synthase subunits were upregulated at 24 h.

Progression of Transcriptional Control

Based on knowledge of the role of TFs in animal stem cells (Takahashi and Yamanaka, 2006), we analyzed TF expression in the protoplast cultures. We extracted lists of TFs and their family annotations from previous reviews (Mitsuda and Ohme-Takagi, 2009; Lu et al., 2012). Of the 5276 DEGs in protoplast culture, 500 TFs were deregulated and assigned to different clusters (see Supplemental Data Set 1 online, columns C to J), a high number (193) of which were deregulated in freshly isolated protoplasts (P0). Our data provide an interesting catalog of putative crucial regulators to be tested for functional roles in cell reprogramming. The 61 TFs stably deregulated in C1 and the 41 TFs in C3 may be essential regulators of cell reprogramming. Most TF families were represented. Interestingly, two families related to the stress response, HFS and TIFY (Vanholme et al., 2007), were only present in C5 (see Supplemental Table 8 online).

The expression profiles of a selection of key genes associated with meristem activity or described as being involved in stem cell maintenance (Yadav et al., 2009; Aichinger et al., 2012) were analyzed (see Supplemental Table 9 online). Among them, we identified *WOUND INDUCED DEDIFFERENTIATION1*, which promotes cell dedifferentiation in *Arabidopsis* (Iwase et al., 2011). Members of the Wuschel-related homeobox (*WOX*) gene family, which are key genes in cell division and prevent premature differentiation (van der Graaff et al., 2009), and of the GRAS gene family (*SHR* and *SCARECROW*), known to be required for the specification and maintenance of the root stem cell niche, were also upregulated. We further compared the DEGs in protoplasts with genes involved in lateral root initiation (Parizot et al., 2010) (see Supplemental Data Set 1, columns BK to BP, and Supplemental Table 10 online). We identified 18 TFs that were deregulated in both our data set and during lateral root initiation, suggesting that there is a partial overlap between these two processes. Among them, *IAA19* and an *ERF* member (*CRF3*) were activated early in protoplasts. Surprisingly, most of the genes were known to be associated with wounding and stress responses. The finding that their expression is maintained during PdC culture might indicate that they have adjacent roles in promoting competence for reentry into the cell cycle and dedifferentiation.

To narrow down the list of key candidate genes in the process, we searched for TF targets of Polycomb proteins and especially of LHP1, a subunit of PRC1 (Zhang et al., 2007; Latrasse et al., 2011). Polycomb proteins are key developmental regulators that repress major developmental genes. We identified 63 TF targets of LHP1, some of which are activated at specific time points and may be key regulators (see Supplemental Table 11 online).

Epigenetic Landscapes of Protoplasts and PdCs in Culture

Since nucleosomes, as substrates for epigenetic modifications and remodelling, are at the heart of gene expression regulation, we analyzed the expression of histone genes during protoplast culture (Talbert et al., 2012) (Table 4). Interestingly, we distinguished sets of histone genes with similar expression. Group A contains genes downregulated at the protoplast stage and activated during the culture with different kinetics. Surprisingly, six H4 genes were expressed during protoplast culture (Table 4). The switch to protoplasts is associated with the transient upregulation of an *H3.3* variant encoded by *HTR8*. These data suggest that protoplast and PdC chromatin have specific properties due to the incorporation of distinct sets of histone variants in nucleosomes.

To characterize the chromatin states of protoplasts and PdCs, we analyzed the ChromDB annotated loci in our data set (see Supplemental Data Set 1, columns K to M, and Supplemental Tables 12 and 13 online). Among them, 108 genes were deregulated in the first five profiles, with major downregulation in protoplasts and a global upregulation at 24 h. The genes were distributed into the eight clusters, C3 being the most abundant, with 25 genes. The genes found in the different clusters encoded proteins involved in histone modification, DNA methylation, and chromatin remodelling (Table 5). Thus, early regulation of the epigenome, specifically through the activation of C3 genes, seems to play an important role in the overall reprogramming of plant cells. It is worth noting the striking similarity with the epigenome plasticity in animal stem cells (Barerro and Izpisua Belmonte, 2011).

PdCs Have Epigenetic Differences from Established Cell Suspensions

It is currently accepted that in vitro culture induces somatic variations, probably involving epigenetic mechanisms. We thus compared the epigenetic status of PdCs to that of a well-established cell suspension. Compared with P168 PdCs, cells in suspension culture had a specific set of histone genes that were upregulated (Groups B and C, Table 4; see Supplemental Table 13 online), whereas *H2A.W.12*, encoding an H2A histone variant, was

Table 4. Transcript Profiles of Histone Genes

AGI	ChromDB	Protein	P0/Pliv	P24/P0	P48/P24	P96/P48	P168/P96	C/P168	C/Pliv	Pliv/Pls	P0/Pls	Group
			1	2	3	4	5	6	7	8	9	
AT5G27670	HTA7	Histone H2A.W.7	nc	nc	nc	nc	**0.76**	nc	nc	nc	*−0.90*	A
AT5G59870	HTA6	Histone H2A.W.6	*−3.53*	nc	**1.44**	**1.52**	**0.69**	**0,71**	nc	nc	*−3.49*	A
AT5G22880	HTB2	Histone HB2.2	*−1.52*	nc	**0.72**	**0.93**	nc	**2.51**	**2.17**	nc	*−1.79*	A
AT5G10390	HTR13	Histone H3.1	*−2.19*	nc	**0.88**	**1.31**	nc	**1.06**	**0.82**	nc	*−2.91*	A
AT2G28740	HFO3	Histone H4	*−2.24*	nc	**1.18**	**1.34**	nc	**1.18**	**1.90**	nc	*−1.91*	A
AT3G46320	HFO1	Histone H4	*−3.09*	−0.82	**1.16**	**1.40**	nc	**2.55**	**1.69**	nc	*−2.86*	A
AT5G59690	HFO2	Histone H4	*−2.88*	−0.62	**0.96**	**1.24**	**0.53**	**1.26**	nc	nc	*−2.98*	A
AT3G54560	HTA11	Histone H2A.Z.11	*−1.47*	nc	nc	**0.73**	nc	nc	nc	nc	*−3.13*	A
AT3G45980	HTB9	Histone H2B.9	*−1.15*	*−1.03*	nc	**0.80**	nc	**1,17**	nc	nc	*−1.18*	A
AT1G07820	HFO4	Histone H4	*−1.85*	nc	nc	**0.72**	nc	**1.24**	**1.03**	nc	*−1.88*	A
AT3G53730	HFO5	Histone H4	nc	*−1.29*	nc	**0.96**	nc	**1.95**	**1.71**	nc	nc	A
AT5G59970	HFO6	Histone H4	*−1.34*	nc	nc	**1.01**	nc	**1.27**	nc	nc	*−1.76*	A
AT2G37470	HTB5	Histone H2B.5	nc	*−1.37*	nc	nc	nc	**1.11**	nc	nc	nc	B
AT2G28720	HTB3	Histone H2B.3	nc	*−1.61*	nc	nc	nc	**2.36**	**1.25**	nc	nc	B
AT2G38810	HTA8	Histone H2A.Z.8	nc	nc	nc	nc	nc	**1.29**	**1.88**	nc	*−1.39*	B
AT5G12910	HTR15	Histone H3.15	*−1.03*	nc	nc	nc	nc	**1.18**	**1.54**	nc	nc	B
AT1G52740	HTA9	Histone H2A.Z.9	nc	nc	nc	nc	nc	**1.27**	nc	nc	nc	C
AT5G54640	HTA1	Histone H2A.1	nc	nc	nc	nc	nc	**1.07**	**1.15**	nc	**0.61**	C
AT4G40030	HTR4	Histone H3.3	nc	nc	nc	nc	nc	**1.70**	nc	nc	nc	C
AT4G40040	HTR5	Histone H3.3	nc	nc	nc	nc	nc	**0.99**	**0.86**	nc	nc	C
AT5G10980	HTR8	Histone H3.3	**1.14**	*−0.87*	nc	nc	nc	**1.60**	**2.00**	nc	**1.05**	D
AT2G18050	HON3	Histone H1.3	nc	nc	nc	nc	nc	nc	nc	nc	**2.23**	D
AT5G02560	HTA12	Histone H2A.W.12	nc	nc	nc	nc	nc	*−1.68*	*−1.41*	nc	nc	E
AT1G07790	HTB1	Histone H2B.1	*−1.66*	nc	nc	nc	nc	nc	nc	nc	*−1.79*	E

Values in bold, upregulated genes; values in italics, downregulated genes; nc, no change in expression.

downregulated. We noticed that numerous other genes associated with chromatin regulation were activated in the cell suspension and identified five new clusters that were specifically deregulated in cell suspension (C10-14; see Supplemental Table 14 and Supplemental Figure 5 online). We also noticed that transposable elements present in the CATMA microarray were reactivated in cell suspension, whereas only two transposable elements were reactivated in PdCs (see Supplemental Table 14 online). Because the microarray used in our analysis was not designed to examine transposable element expression profiles, we expect that many more transposable elements are deregulated in cell suspension.

The floral repressor gene *FWA*, which is silenced in adult tissues and subjected to imprinting, was also specifically reactivated in this established cell suspension. *ROS1*, involved in active DNA demethylation, was also upregulated in cell suspension, as was *DRM1*, which is involved in de novo DNA methylation, suggesting that major changes in methylation status occur due to prolonged cell culture. In addition, key genes in silencing mechanisms (i.e., *AGO5*, *DCL3*, and *HEN1*) were also activated. Thus, small RNA regulation appeared to be differently affected in cell suspension compared with PdCs. Therefore, PdCs were epigenetically closer to plants than to a cell suspension, suggesting that PdCs maintained epigenetic imprinting despite dedifferentiation events and reentry into the cell cycle.

The Roles of AGO4 and ALF4 during Protoplast Culture

Given that the first day in culture is crucial for the development of the protoplast, we tested the functional roles of two genes upregulated at 24 h: *ABERRANT LATERAL ROOT FORMATION4* (*ALF4*) in C3 and *ARGONAUTE4* (*AGO4*) in C6. Since DNA hypermethylation correlates with reprogramming efficiency in animal somatic cells (Barrero et al., 2012), and knowing the essential role of *PIWI* genes in maintaining germ line cells and stem cell properties (stemness) (Alié et al., 2011), we were intrigued by the early upregulation of *AGO4*. Protoplasts of homozygous *ago4-4* mutant plantlets were able to divide, revealing that AGO4 is not essential for the reentry into cell division. There is functional redundancy between AGO4 and AGO9 (Elmayan et al., 2005; Mallory and Vaucheret, 2010); thus, it remains to be tested whether *ago9* and *ago4 ago9* protoplasts are able to reenter the cell division cycle.

Initially identified as regulating the formation of lateral roots (Celenza et al., 1995; DiDonato et al., 2004), *ALF4* is also essential for callus formation from pericycle cells of *Arabidopsis* explants (Sugimoto et al., 2010). Under binocular loupe, *alf4-1* homozygous plants were strictly selected based on their morphological root phenotype (see Supplemental Figure 6 online). Protoplasts prepared from homozygous *alf4-1* plantlets were unable to divide, except for about one in 10^4 protoplasts, which were probably derived from either rare heterozygous seedlings or wild-type seedlings retarded in lateral root development. Furthermore, nondividing *alf4* protoplasts were fully viable and could condition the culture medium, thus supporting colony formation for the rare PdCs of other genotypes. These data demonstrate that *ALF4* is necessary for protoplast division. This finding expands the role of *ALF4* to every cell type, highlighting its crucial involvement in the reinitiation of cell division in tissues beyond the meristem.

Table 5. DEGs of the Eight Main Clusters Involved in Chromatin Regulation

Cluster	AGI	Selection	ChromDB ID/Formal Name
C1	AT3G51000	α/β-Hydrolases superfamily	ABHF10
	AT5G64630	Nucleosome/chromatin assembly complex	NFB1/FAS2
	AT1G08620	Jumonji domain group	JMJ16
C2	AT4G37470	α/β-Hydrolases superfamily protein	ABHF2
	AT5G49160	DNA methyltransferase	DMT1/DDM2/MET1
	AT3G15790	Methyl binding domain protein	MBD11
	AT5G41070	Double stranded RNA binding protein group	DRB5
	AT5G63670	Transcription elongation-nucleosome displacement protein	GTG1
	AT1G14900	HMG group family	HMGA3
	AT1G76110	HMG group family	HMGB9
C3	AT3G03990	α/β-Hydrolases superfamily protein	ABHF1
	AT2G17410	ARID/BRIGHT DNA binding domain-containing protein	ARID3
	AT1G08600	Chromatin remodeling complex	CHR20
	AT5G19310	Chromatin remodeling complex	CHR23
	AT4G26110	Nucleosome/chromatin assembly complexes	NFA1/NAP1
	AT5G58230	Nucleosome/chromatin assembly complex	NFC1/MSI1
	AT5G67630	ATPase/helicase	RUVBL2
	AT2G27170	Structural maintenance of chromosomes family protein	CPC5/TTN7
	AT3G17310	DNA methyltransferase	DMT10/DRM3
	AT5G46550	Global TF	GTE12
	AT4G38130	Histone deacetylase	HDA19/D1
	AT3G44750	Histone deacetylase	HDT1/HD2A/HDA3
	AT5G03740	Histone deacetylase	HDT3/HD2C/HDA11
	AT1G55255	Histone ubiquitination protein	HUPA2/HUB2
	AT3G48430	Jumonji domain group	JMJ12/REF6
	AT4G20400	Jumonji domain group	JMJ14
	AT2G38950	Jumonji domain group	JMJ19
	AT5G04940	SET domain protein	SDG32/SUVH1
	AT5G13960	SET domain protein	SDG33/SUVH4
	AT1G01920	SET domain protein	SDG42/SDG42
	AT4G29510	Protein Arg methyltransferase	PRMT11/PAM1
	AT1G79730	PAF1 complex	PAFA1/ELF7
	AT3G49660	COMPASS complex	SWDC2
	AT1G45000	Proteasomal ATPase	PATPA2
	AT5G23570	Suppressor of gene silencing	SGS3
C4	AT5G19850	α/β-Hydrolases superfamily protein	ABHF9
	AT1G15340	Methyl binding domain protein	MBD10
	AT5G03220	Mediator subunit	MED7SUB2
	AT1G14400	Histone ubiquitination protein	HUPB1/UBC1
	AT5G09230	Histone deacetylase	SRT2
C5	AT2G02760	Histone ubiquitination protein	HUPB2/UBC2
	AT5G46910	Jumonji domain group	JMJ13
	AT1G26665	Mediator subunit	MED10SUB2
	AT1G55080	Mediator subunit	MED9SUB1
	AT1G17520	Single myb histone protein group	SMH13
C6	AT2G27040	Argonaute family protein	AGO4
	AT3G17590	Chromatin remodeling complex	CHE1/BSH
	AT3G46580	Methyl binding domain protein	MBD5
	AT2G19520	NURF complex	NFC4/FVE
	AT5G49020	Protein Arg methyltransferase	PRMT4a
	AT5G38110	Antisilencing function 1b	SGA1
	AT1G49480	Transcription regulation (VRN1 homolog)	VPGA2
C7	AT5G62410	Condensin complex	CPC3/TTN3
C8	AT5G43810	Argonaute family protein	AGO10/PNH
	AT2G25170	Chromatin remodeling complex	CHR6/PKL
	AT3G47460	Structural maintenance of chromosomes family protein	CPC4/SMC2
Various	AT1G58025	Bromodomain containing protein	BRD5
	AT4G11130	RNA-dependent RNA polymerase	RDR2
	AT1G18800	Nucleosome/chromatin assembly complex	NFA5/NRP2
	AT5G06550	Jumonji domain group	JMJ22
	AT5G22650	Histone deacetylase	HDT2/HD2B
	AT2G19640	SET domain protein	SDG39/ASHR2
	AT2G17900	SET domain protein	SDG37/ASHR1

DISCUSSION

Large populations of homogenized plant cells can be obtained overnight and easily handled in liquid culture under conditions determined in this study to yield a large fraction of cells that reenter the cell cycle. The flexibility and efficiency of the protoplast system developed here provides a useful tool for examining the fundamental processes of reentry into the cell cycle and totipotency. Furthermore, the high frequency of bud regeneration may be used to characterize the early molecular events underlying meristem formation.

Transcript profiling at various time points during the preparation and culture of protoplasts revealed 5276 deregulated genes. With next-generation sequencing approaches, this number could certainly increase, which would allow us to investigate the regulatory roles of noncoding RNAs in this process. The deregulated genes were organized into eight main gene clusters with specific GO patterns that suggest sequential transcriptional phases and an apparent synchronization of reentry into the cell cycle for most PdCs in culture. The temporal profiling conducted here has yielded much data that can be used in future studies. Thus, protoplast dedifferentiation provides a simple and homogeneous experimental cell system as an alternative to in planta activation of tissue-specific cell division, which is involved in transdifferentiation or differentiation of precursor cells (Sena and Birnbaum, 2010; Sugimoto et al., 2011).

During protoplast isolation and the early culture steps, dedifferentiation occurred rapidly and affected all cell types originating from the aerial parts of plantlets. Dedifferentiation resulted from the massive degradation of various cellular constituents (e.g., proteins, the cell wall, and the photosynthetic apparatus) by repression of the underlying genes and transcriptional reorientation, and the activation of numerous TFs and posttranscriptional controls.

Protein synthesis pathways were notably repressed by protoplasting, with all of the ribosomal protein genes being downregulated, in agreement with the low number of ribosomes observed in tobacco protoplasts by microscopy analysis (Gigot et al., 1975). Once protoplasts were cultured, protein synthesis was reactivated (Zelcer and Galun, 1976). We show a clear reorientation of protein synthesis toward cell division. Identifying the ribosomal equipment needed at specific stages to regulate reentry into the cell cycle will require further studies; however, the importance of RPs in gene expression and development have been reported (Byrne, 2009; Kondrashov et al., 2011). We identified a specific cell cycle cluster containing genes upregulated at 96 h, consistent with microscopy observations of divisions in culture.

Our study revealed a complex array of 500 TF profiles during the early steps of establishing totipotency. Some TF families, such as the Tify and HFS families, were associated with specific clusters and therefore are good markers of particular time points, whereas the members of other families were activated at different time points in the process. Because the early dedifferentiation events are critical for reentry into the cell cycle, an analysis of TFs activated in protoplasts after 0 and 24 h in culture (C1 and C3, respectively) will help to elucidate the transcriptional network underlying totipotency. For example, of all the TFs activated in C1, only 26 were not expressed during senescence. These 26 TFs may be crucial for dedifferentiation and the acquisition of basal competence for cell division. The 34 TFs of C3 not deregulated during senescence may be involved in the core transcriptional regulatory network underlying totipotency. Further comparisons with studies conducted in other species will help identify which TFs are crucial for establishing totipotency.

Numerous TFs with known meristematic or stem cell functions, such as the three members of the WOX family, were deregulated during the establishment of totipotency. *WOX5* is an auxin-inducible gene expressed in the quiescent center of the root meristem and in its direct precursor cells during the early globular stage of embryogenesis (Haecker et al., 2004; Gonzali et al., 2005). *WOX8* is expressed in the egg cell and zygote, whereas *WOX13* is expressed during primary and lateral root initiation and development, in the gynecium, and during embryo development (Deveaux et al., 2008; Romera-Branchat et al., 2012). The sequential reactivation of *WOX13*, *WOX5*, and then *WOX8* suggests that these genes are also regulators of cell division during PdC culture. Surprisingly, genes encoding TFs specific to embryo development (*LEC1*), leaf development (*PHB*), and floral development (*PI* and *SVP*) were transiently activated, also suggesting that these genes have broader functions than reported previously. We found that *ALF4*, in addition to its well-characterized role in lateral root initiation (Celenza et al., 1995; DiDonato et al., 2004) and callus formation (Sugimoto et al., 2010), is crucial for the reentry of protoplasts into the cell cycle.

We observed striking similarities between animal cell reprogramming and the early developmental events of *Arabidopsis* protoplasts in culture, highlighting some degree of conservation of reprogramming processes. The dedifferentiation of protoplasts, which is accompanied by stress responses (Grafi et al., 2011), is reminiscent of inflammatory reactions in animal cells (Barrero and Izpisua Belmonte, 2011; Lee et al., 2012). PdCs reacted to hypoxia by shifting to glycolysis. In animal cells, a similar shift toward energy production by glycolysis is a distinctive trait of the transition from differentiated cells to stem cells (Zhang et al., 2011; Zhou et al., 2012). We highlighted major changes in chromatin-related gene expression, suggesting that chromatin has a specific composition in protoplasts and PdCs, with specific sets of histone variants and histone posttranslational modifications. Thus, in *Arabidopsis*, dedifferentiation and further steps toward PdC development require extensive epigenetic reprogramming reminiscent of animal stem cell reprogramming (Barrero and Izpisua Belmonte, 2011; Jullien et al., 2012; Solana et al., 2012). The genome-wide transcriptional reorientation we observed in this study confirmed the large-scale chromatin rearrangements we previously described at the microscopic and cytological levels (Tessadori et al., 2007). A number of LHP1 targets were deregulated throughout the entire process, suggesting that Polycomb complexes are also involved in the early regeneration steps from isolated somatic cells and expanding their roles to include the regulation of cell fate and differentiation (Köhler and Hennig, 2010). Interestingly, the nature of epigenetic reprogramming differed from the epigenetic modifications observed in a well-established cell suspension not undergoing organogenesis. The maintenance of imprinted genes, such as *FWA*,

and of transposons in a silent state in PdCs is consistent with the absence of activation of silent transgenes in protoplasts, despite chromatin decondensation (Tessadori et al., 2007). Our data suggest that silencing is maintained in PdCs, but not in cell suspension.

In our study, only a few genes specific to particular developmental stages (e.g., root, meristem, and embryo development) were upregulated during protoplast culture. These observations suggest that these genes have broader functions than previously thought. Furthermore, they show that totipotent protoplasts and the derived cells develop in response to unique and complex combinations of molecular and metabolic signatures. The assumption that animal stem cell identity is more a product of the transient, specific molecular and metabolic status of the cell than of cellular identity (Zipori, 2004) seems to apply well to the totipotency of plant cells.

METHODS

Plant Materials and Growth Conditions

Seeds of *Arabidopsis thaliana* Col-0 and Ws accessions were obtained from the Institut National de la Recherche Agronomique Versailles Genetics and Plant Breeding Laboratory (Arabidopsis Resource Centre). Disinfectant solution was prepared by dissolving a pill of sodium dichloroisocyanurate (Bayrol) in 40 mL water and adding 160 mL ethanol. Seeds (20 mg) were disinfected in 1 mL of disinfectant solution in an Eppendorf tube for 10 min, rinsed twice with ethanol, and left to dry overnight. Approximately 250 seeds were sown on 75 mL GM (see Supplemental Table 1, online) in green boxes (Kalys), and placed at 4°C for 2 to 3 d. To cultivate plantlets in soil, seeds were sown directly on compost covered with a thin vermiculite layer and watered with GM as for in vitro culture, but in the absence of Suc. Plantlets were cultivated in soil or in vitro on plates of medium under 10 h light, 75% relative air humidity, at 20°C. A mix of Biolux and plain white light tubes were used, giving an average light intensity of 50 $\mu Es^{-1}\ s^{-1}\ m^2$. The light intensity at the level of the leaves of plants grown in vitro was around 30 $\mu Es^{-1}\ s^{-1}\ m^2$. PSB-L *Arabidopsis* cells (May and Leaver, 1993) were cultured according to De Sutter et al. (2005).

Seeds from the heterozygous *afl4-1* mutant in the Col-0 accession background (a gift from John Celenza) were sown in large Petri dishes (diameter, 145 mm), at a low density (40 seeds per dish) on GM. Based on the developmental phenotype, homozygous plantlets without secondary roots were selected for protoplast isolation (see Supplemental Figure 6 online). Plantlets were selected under binocular loupe. Of 964 seedlings, 139 plantlets without lateral roots were selected (far fewer than the expected 241 homozygous mutants) and used to isolate 5×10^6 *alf4-1*−/− protoplasts.

Protoplast Isolation and Culture

Optimal protoplast yield and viability were obtained using maceration medium that contained Gly and Glc as osmotic agents (MGG; see Supplemental Table 1 online). Approximately 0.6 g of the aerial parts of 3-week-old sterile plantlets (at the four to six leaf stage) was soaked in 5 mL of maceration medium in a Petri dish (see Supplemental Table 1 online) to prevent drying and rapidly chopped. Five milliliters of MGG was added, bringing the total volume to 10 mL. Maceration was performed in the dark, at 24°C, overnight. Due to the toxicity of ammonium ions in culture, the mineral composition of the maceration medium was adjusted to 0.2 mM ammonium (MGG; see Supplemental Table 1 online). After cell wall digestion, 20 mL protoplast suspension in MGG was filtered through an autoclaved 80-μm mesh filter, over 10 mL washing solution (2.5% KCl and 0.2% $CaCl_2$) already added to a 30-mL glass tube. After centrifugation (70*g*, 6 min), protoplast pellets were gently resuspended in 25 mL washing solution and centrifuged again (70*g*, 6 min). Washing was performed two more times. This procedure allowed for the collection of protoplasts isolated from most cell types. Protoplast numbers were estimated on a Malassez slide from an aliquot of the resuspended suspension before the last centrifugation. Approximately 4.5×10^7 viable protoplasts were routinely isolated from plantlets cultured in six green boxes. After a 1-h incubation at 4°C in tubes in a volume of washing medium just enough to cover the pellet, the protoplast suspension was diluted in PIM to a concentration of 8×10^5 protoplasts per milliliter. One milliliter of protoplast suspension in PIM was then added to 9 mL PIM already present in Petri dishes to reach the starting density of 8×10^4/mL. Liquid media (PIM, colony induction medium 1, and colony induction medium 2; see Supplemental Table 1 online) were supplemented with 10 μL/L Tween 80 to facilitate the wetting of plastic dishes and thus prevent the bursting of plated protoplasts. All media were autoclaved for 20 min at 115°C, and growth substances and $FeCitrateNH_4$ were added in a sterile manner after autoclaving. The plates were subsequently placed in large plastic boxes to limit evaporation, and cell suspensions were cultured in the dark at 20°C. The suspensions were diluted as described in Results to regenerate plantlets from the PdC suspensions. The cell division rate was estimated by counting the number of dividing protoplasts on a Malassez slide under a light microscope.

RNA Extraction and Microarray Data

RNAs from 3-week-old seedlings, protoplasts, and PdCs after 24, 48, 96, and 168 h of culture were extracted using the RNAeasy mini kit (Qiagen). RNA integrity was tested with an Agilent Bioanalyzer. For each biological replicate, 4.5×10^7 protoplasts were isolated: 10^7 of freshly prepared protoplasts were used for time point 0 h, and 3×10^7 protoplasts were dispatched and cultured in 40 Petri dishes (8×10^5 per dish). Cells from nine Petri dishes were pooled for each culture time point. Hybridization microarray analysis and statistical analyses based on two independent biological replicates, and two dye-swaps were performed as previously described using the 25 K CATMA_v2.1 microarray bearing 24 576 gene-specific tags (Lurin et al., 2004; Gagnot et al., 2008) (see Supplemental Methods 1 online).

After statistical validation, variations in transcript abundance were expressed as the $\log_2$ of the ratio of hybridization intensities between biological materials and/or successive steps. The microarray data sets were deposited into the Gene Expression Omnibus (http://www.ncbi.nlm.nih.gov/geo/; accession number GSE7984) and CATdb (http://urgv.evry.inra.fr/cgi-bin/projects/CATdb/consult_project.pl?project_id=28.), according to Minimum Information About a Microarray Experiment standards.

Transcriptome Analysis

Supplemental Data Set 1 online lists the 8206 genes differentially expressed in at least one of the nine conditions tested in our experimental design. The various publicly available data sets used in this study, such as the chromatin-related genes (ChromDB; http://chromdb.org/), the lists of TFs (Mitsuda and Ohme-Takagi, 2009; Lu et al., 2012), and the list of genes from Visual LRTC (Parizot et al., 2010), were merged with our transcript profiles, our lists of genes associated with selected GO information related to the cell wall and cell cycle (GO website), and the identity of the clusters. A specific spreadsheet in Supplemental Data Set 1 online, called gene selector, was designed in Excel using advanced functions, to extract expression profiles and information related to small user lists of sorted AGIs. The function was updated with the latest version

available on TAIR (TAIR10_functional_descriptions, 23/08/2011 version, Columnumn Short_description).

BAR (http://www.bar.utoronto.ca/) and its Classification SuperViewer Tool (Provart et Zhu, 2003), based on the GO functional classifications (January 5, 2010; file ATH_GO_GOSLIM.20100105), was used to calculate normed frequencies of the classes, bootstrap standard deviations, and P values. EasyGO (GO enrichment analysis tool, http://bioinformatics.cau.edu.cn/easygo/) and agriGO (Du et al., 2010) were also used for detailed analysis of GO term enrichment. Genes related to the cell cycle (GO:0007049, GO:0051301, GO:0000910, and GO:0000280) and cell wall elaboration (GO:0071554 and GO:0009664) were extracted from AmiGO (http://amigo.geneontology.org/cgi-bin/amigo/go.cgi; all-association files: gene products annotated to the GO term or any of its children). Clustering and visualization of the gene expression differences were performed using the Multiexperiment Viewer tool. Hierarchical clustering was done using the Euclidean distance metric and average linkage clustering as the linkage method (Saeed et al., 2003). Venn diagrams were constructed using the tool Venn diagrams from Gent University (http://bioinformatics.psb.ugent.be/webtools/Venn/).

Accession Numbers

Sequence data from this article can be found in the Arabidopsis Genome Initiative under the accession numbers presented in Supplemental Data Set 1 online. The microarray data sets were deposited into the Gene Expression Omnibus (http://www.ncbi.nlm.nih.gov/geo/) under accession number GSE7984.

Supplemental Data

The following materials are available in the online version of this article.

Supplemental Figure 1. Clustering of the Transcript Profiles.

Supplemental Figure 2. Venn Diagram Showing the Distribution of DE5 Genes Isolated in Our Study and Known to Be Expressed during Senescence and to Be Involved in Stress Responses.

Supplemental Figure 3. Venn Diagram Showing Common Genes Deregulated in Protoplast Transcriptomes Established in Our Study and in Two Previous Studies.

Supplemental Figure 4. The Expression of *A. thaliana* Cell Cycle Genes at Various Time Points during Protoplast Culture.

Supplemental Figure 5. Venn Diagram Highlighting Genes Specific to Cell Suspension (Common in C/P168 and C/Pliv) or to the Protoplast Stage (Only Deregulated in P0/Pliv).

Supplemental Figure 6. Phenotype of the *alf4-1* Mutant.

Supplemental Table 1. Media Compositions for *A. thaliana* Protoplast Culture (mg/L).

Supplemental Table 2. Validation of Microarray Data.

Supplemental Table 3. Complete GO Descriptions of the Eight Main Clusters Identified in This Study.

Supplemental Table 4. List of DEGs Common to Our Study (P0/Pliv) and Two Previous Studies (Damri et al., 2009; Yadav et al., 2009).

Supplemental Table 5. List of DEGs Deregulated in DE5 (5276 Total Genes) and Present among the 70 Genes Involved in Meristem (Yadav et al., 2009).

Supplemental Table 6. List DEGs Deregulated in Pliv/P0 (This Work), Meristem Protoplasts (Yadav et al., 2009), and Moss Protoplasts (Xiao et al., 2012).

Supplemental Table 7. Expression Profiles of Auxin-Related Genes at Various Time Points in *A. thaliana* Protoplast Culture.

Supplemental Table 8. Selected TF Families and Their Distribution in the Eight Clusters Identified in This Study.

Supplemental Table 9. Expression Profiles of Selected TFs Involved in Developmental Processes.

Supplemental Table 10. Transcription Factors Involved in Lateral Root Initiation (Parizot et al., 2010) and Deregulated in Our Study.

Supplemental Table 11. Transcription Factor Targets of LHP1 That Were Deregulated in Our Study.

Supplemental Table 12. Distribution of the 559 ChromDB Genes Deregulated in Our Study and in the Eight Main Clusters.

Supplemental Table 13. The ChromDB Genes Deregulated in *A. thaliana* Cell Suspension Form Five New Clusters.

Supplemental Table 14. Expression Profiles of Transposable Elements during *A. thaliana* Protoplast Culture Compared with Cell Suspension (C) Culture.

Supplemental Methods 1. Transcriptome Hybridization, Data Analysis and qRT-PCR.

Supplemental References 1. References for Supplemental Figures 2 and 3 and Supplemental Tables 1, 4, 5, and 6.

Supplemental Data Set 1. Excel File Containing Expression Profiles, Annotations, and the Gene Selector Tool, for Extraction from These Data Sets of a Given Gene or Set of Genes in the Process of Cell Reprogramming.

ACKNOWLEDGMENTS

This work was supported by the Institut National de la Recherche Agronomique, France. We thank John Celenza for *afl4-1* seeds, Hervé Vaucheret for *ago4-4* seeds and fruitful discussions, and all technicians in charge of the Institut Jean-Pierre Bourgin greenhouses, with special mention to Bruno Letarnec. We thank Carolyn Napoli and the Chromatin Database for providing the *Arabidopsis* chromatin gene list, Boris Parizot for providing the VisuaLRTC Excel module, and Chi Zhang for the list of TFs and their families. We also thank Margaret Platt-Hommel, Herman Höfte, and Loïc Lepiniec for critical reading of the article.

AUTHOR CONTRIBUTIONS

M.-C.C., Y.C., and V.G. conceived and designed the experiments. M.-C.C., V.G., and O.P. performed the experiments. O.P., J.-P.R., F.G., V.G., and Y.C. analyzed the data. V.G. and Y.C. wrote the article.

Received January 15, 2013; revised May 31, 2013; accepted July 3, 2013; published July 31, 2013.

REFERENCES

Aichinger, E., Kornet, N., Friedrich, T., and Laux, T. (2012). Plant stem cell niches. Annu. Rev. Plant Biol. **63:** 615–636.

Alié, A., Leclère, L., Jager, M., Dayraud, C., Chang, P., Le Guyader, H., Quéinnec, E., and Manuel, M. (2011). Somatic stem cells express Piwi and Vasa genes in an adult ctenophore: Ancient association of "germline genes" with stemness. Dev. Biol. **350:** 183–197.

Aremu, A.O., Bairu, M.W., Doležal, K., Finnie, J.F., and Staden, J. (2012). Topolins: A panacea to plant tissue culture challenges? Plant Cell Tissue Organ Cult. **108:** 1–16.

Atta, R., Laurens, L., Boucheron-Dubuisson, E., Guivarc'h, A., Carnero, E., Giraudat-Pautot, V., Rech, P., and Chriqui, D. (2009). Pluripotency of *Arabidopsis* xylem pericycle underlies shoot regeneration from root and hypocotyl explants grown in vitro. Plant J. **57:** 626–644.

Atias, O., Chor, B., and Chamovitz, D.A. (2009). Large-scale analysis of *Arabidopsis* transcription reveals a basal co-regulation network. BMC Syst. Biol. **3:** 86.

Barakat, A., Szick-Miranda, K., Chang, I.F., Guyot, R., Blanc, G., Cooke, R., Delseny, M., and Bailey-Serres, J. (2001). The organization of cytoplasmic ribosomal protein genes in the *Arabidopsis* genome. Plant Physiol. **127:** 398–415.

Barrero, M.J., Berdasco, M., Paramonov, I., Bilic, J., Vitaloni, M., Esteller, M., and Izpisua Belmonte, J.C. (2012). DNA hypermethylation in somatic cells correlates with higher reprogramming efficiency. Stem Cells **30:** 1696–1702.

Barrero, M.J., and Izpisua Belmonte, J.C. (2011). Regenerating the epigenome. EMBO Rep. **12:** 208–215.

Bourgin, J.P., Chupeau, Y., and Missonier, C. (1979). Plant regeneration from mesophyll protoplasts of several Nicotiana species. Physiol. Plant. **45:** 288–292.

Breeze, E., et al. (2011). High-resolution temporal profiling of transcripts during *Arabidopsis* leaf senescence reveals a distinct chronology of processes and regulation. Plant Cell **23:** 873–894.

Byrne, M.E. (2009). A role for the ribosome in development. Trends Plant Sci. **14:** 512–519.

Buchanan-Wollaston, V., Page, T., Harrison, E., Breeze, E., Lim, P.O., Nam, H.G., Lin, J.F., Wu, S.H., Swidzinski, J., Ishizaki, K., and Leaver, C.J. (2005). Comparative transcriptome analysis reveals significant differences in gene expression and signalling pathways between developmental and dark/starvation-induced senescence in *Arabidopsis*. Plant J. **42:** 567–585.

Caboche, M. (1980). Nutritional requirements of protoplast derived, haploid tobacco cell grown at low cell densities in liquid medium. Planta **149:** 7–18.

Candela, M., and Velazquez, I. (2001). Differences in plant regeneration *in vitro* among four *Arabidopsis* ecotypes. In Vitro Cell. Dev. Biol. Plant **37:** 638–643.

Celenza, J.L., Jr., Grisafi, P.L., and Fink, G.R. (1995). A pathway for lateral root formation in *Arabidopsis thaliana*. Genes Dev. **9:** 2131–2142.

Chang, B.Y., Harte, R.A., and Cartwright, C.A. (2002). RACK1: A novel substrate for the Src protein-tyrosine kinase. Oncogene **21:** 7619–7629.

Chantha, S.-C., Emerald, B.S., and Matton, D.P. (2006). Characterization of the plant Notchless homolog, a WD repeat protein involved in seed development. Plant Mol. Biol. **62:** 897–912.

Chantha, S.C., Tebbji, F., and Matton, D.P. (2007). From the notch signaling pathway to ribosome biogenesis. Plant Signal. Behav. **2:** 168–170.

Chupeau, M.C., Lemoine, M., and Chupeau, Y. (1993). Requirement of thidiazuron for healthy protoplast development to efficient tree regeneration of a hybrid Poplar (*P. tremula* x *P. alba*). J. Plant Physiol. **141:** 601–609.

Chupeau, Y., Bourgin, J.P., Missonier, C., Dorion, N. and Morel, G. (1974). Préparation et culture de protoplastes de divers *Nicotiana*. C. R. Acad. Sci. Paris D **278:** 1565–1568.

Crowe, M.L., et al. (2003). CATMA: A complete *Arabidopsis* GST database. Nucleic Acids Res. **31:** 156–158.

Cui, X., Fan, B., Scholz, J., and Chen, Z. (2007). Roles of *Arabidopsis* cyclin-dependent kinase C complexes in cauliflower mosaic virus infection, plant growth, and development. Plant Cell **19:** 1388–1402.

Damm, B., and Willmitzer, L. (1988). Regeneration of fertile plants from protoplasts of different *Arabidopsis thaliana* genotypes. Mol. Gen. Genet. **213:** 15–20.

Damri, M., Granot, G., Ben-Meir, H., Avivi, Y., Plaschkes, I., Chalifa-Caspi, V., Wolfson, M., Fraifeld, V., and Grafi, G. (2009). Senescing cells share common features with dedifferentiating cells. Rejuvenation Res. **12:** 435–443.

Davey, M.R., Anthony, P., Power, J.B., and Lowe, K.C. (2005). Plant protoplasts: Status and biotechnological perspectives. Biotechnol. Adv. **23:** 131–171.

Demidov, D., Van Damme, D., Geelen, D., Blattner, F.R., and Houben, A. (2005). Identification and dynamics of two classes of aurora-like kinases in *Arabidopsis* and other plants. Plant Cell **17:** 836–848.

De Smet, I., et al. (2008). Receptor-like kinase ACR4 restricts formative cell divisions in the *Arabidopsis* root. Science **322:** 594–597.

De Sutter, V., Vanderhaeghen, R., Tilleman, S., Lammertyn, F., Vanhoutte, I., Karimi, M., Inze, D., Goossens, A., and Hilson, P. (2005). Exploration of jasmonate signalling via automated and standardized transient expression assays in tobacco cells. Plant J. **44:** 1065–1076.

Deveaux, Y., Toffano-Nioche, C., Claisse, G., Thareau, V., Morin, H., Laufs, P., Moreau, H., Kreis, M., and Lecharny, A. (2008). Genes of the most conserved WOX clade in plants affect root and flower development in *Arabidopsis*. BMC Evol. Biol. **8:** 291.

Dewitte, W., and Murray, J.A. (2003). The plant cell cycle. Annu. Rev. Plant Biol. **54:** 235–264.

DiDonato, R.J., Arbuckle, E., Buker, S., Sheets, J., Tobar, J., Totong, R., Grisafi, P., Fink, G.R., and Celenza, J.L. (2004). *Arabidopsis* ALF4 encodes a nuclear-localized protein required for lateral root formation. Plant J. **37:** 340–353.

Dovzhenko, A., Dal Bosco, C., Meurer, J., and Koop, H.U. (2003). Efficient regeneration from cotyledon protoplasts in *Arabidopsis thaliana*. Protoplasma **222:** 107–111.

Du, Z., Zhou, X., Ling, Y., Zhang, Z., and Su, Z. (2010). agriGO: A GO analysis toolkit for the agricultural community. Nucleic Acids Res. **38** (Web Server issue)**:** W64–W70.

Elmayan, T., Proux, F., and Vaucheret, H. (2005). *Arabidopsis* RPA2: A genetic link among transcriptional gene silencing, DNA repair, and DNA replication. Curr. Biol. **15:** 1919–1925.

Eisenberg, T., et al. (2009). Induction of autophagy by spermidine promotes longevity. Nat. Cell Biol. **11:** 1305–1314.

Fujii, S., and Small, I. (2011). The evolution of RNA editing and pentatricopeptide repeat genes. New Phytol. **191:** 37–47.

Gagnot, S., Tamby, J.-P., Martin-Magniette, M.-L., Bitton, F., Taconnat, L., Balzergue, S., Aubourg, S., Renou, J.-P., Lecharny, A., and Brunaud, V. (2008). CATdb: A public access to *Arabidopsis* transcriptome data from the URGV-CATMA platform. Nucleic Acids Res. **36** (Database issue)**:** D986–D990.

Giavalisco, P., Wilson, D., Kreitler, T., Lehrach, H., Klose, J., Gobom, J., and Fucini, P. (2005). High heterogeneity within the ribosomal proteins of the *Arabidopsis thaliana* 80S ribosome. Plant Mol. Biol. **57:** 577–591.

Gil, P., Dewey, E., Friml, J., Zhao, Y., Snowden, K.C., Putterill, J., Palme, K., Estelle, M., and Chory, J. (2001). BIG: A calossin-like protein required for polar auxin transport in *Arabidopsis*. Genes Dev. **15:** 1985–1997.

Gigot, C., Kopp, M., Schmitt, C., and Milne, R. (1975). Subcellular changes during isolation and culture of tobacco mesophyll protoplasts. Protoplasma **84:** 31–41.

González, F., Boué, S., and Izpisúa Belmonte, J.C. (2011). Methods for making induced pluripotent stem cells: Reprogramming à la carte. Nat. Rev. Genet. **12:** 231–242.

Grafi, G., Chalifa-Caspi, V., Nagar, T., Plaschkes, I., Barak, S., and Ransbotyn, V. (2011). Plant response to stress meets dedifferentiation. Planta **233:** 433–438.

Gonzali, S., Novi, G., Loreti, E., Paolicchi, F., Poggi, A., Alpi, A., and Perata, P. (2005). A turanose insensitive mutant suggests a role for WOX5 in auxin homeostasis in Arabidopsis thaliana. Plant J. **44:** 633–645.

Guo, J., Wang, S., Valerius, O., Hall, H., Zeng, Q., Li, J.F., Weston, D.J., Ellis, B.E., and Chen, J.G. (2011). Involvement of *Arabidopsis* RACK1 in protein translation and its regulation by abscisic acid. Plant Physiol. **155:** 370–383.

Gutierrez, C. (2009). The *Arabidopsis* cell division cycle. In The Arabidopsis Book **7:** e0120, doi/10.1199/tab.0120.

Haecker, A., Gross-Hardt, R., Geiges, B., Sarkar, A., Breuninger, H., Herrmann, M., and Laux, T. (2004). Expression dynamics of WOX genes mark cell fate decisions during early embryonic patterning in *Arabidopsis thaliana*. Development **131:** 657–668.

He, C., Chen, X., Huang, H., and Xu, L. (2012). Reprogramming of H3K27me3 is critical for acquisition of pluripotency from cultured *Arabidopsis* tissues. PLoS Genet. **8:** e1002911.

Heller, R. (1953). Recherches sur la nutrition minérale des tissus végétaux cultivés in vitro. Ann. Sci. Nat. Bot. Biol. Veg. **14:** 1–223.

Hilson, P.J., et al. (2004). Versatile gene-specific sequence tags for *Arabidopsis* functional genomics: Transcript profiling and reverse genetics applications. Genome Res. **14** (10B)**:** 2176–2189.

Holec, S., Lange, H., Kühn, K., Alioua, M., Börner, T., and Gagliardi, D. (2006). Relaxed transcription in *Arabidopsis* mitochondria is counterbalanced by RNA stability control mediated by polyadenylation and polynucleotide phosphorylase. Mol. Cell. Biol. **26:** 2869–2876.

Horii, M., and Marubashi, W. (2005). Even juvenile leaves of tobacco exhibit programmed cell death. Plant Biotechnol. **22:** 339–344.

Iwase, A., Mitsuda, N., Koyama, T., Hiratsu, K., Kojima, M., Arai, T., Inoue, Y., Seki, M., Sakakibara, H., Sugimoto, K., and Ohme-Takagi, M. (2011). The AP2/ERF transcription factor WIND1 controls cell dedifferentiation in *Arabidopsis*. Curr. Biol. **21:** 508–514.

Jopling, C., Boue, S., and Izpisua Belmonte, J.C. (2011). Dedifferentiation, transdifferentiation and reprogramming: Three routes to regeneration. Nat. Rev. Mol. Cell Biol. **12:** 79–89.

Jullien, J., Astrand, C., Szenker, E., Garrett, N., Almouzni, G., and Gurdon, J.B. (2012). HIRA dependent H3.3 deposition is required for transcriptional reprogramming following nuclear transfer to Xenopus oocytes. Epigenetics Chromatin **5:** 17.

Kende, H., Bradford, K., Brummell, D., Cho, H.-T., Cosgrove, D., Fleming, A., Gehring, C., Lee, Y., McQueen-Mason, S., Rose, J., and Voesenek, L.A.C.J. (2004). Nomenclature for members of the expansin superfamily of genes and proteins. Plant Mol. Biol. **55:** 311–314.

Köhler, C., and Hennig, L. (2010). Regulation of cell identity by plant Polycomb and trithorax group proteins. Curr. Opin. Genet. Dev. **20:** 541–547.

Kondrashov, N., Pusic, A., Stumpf, C.R., Shimizu, K., Hsieh, A.C., Xue, S., Ishijima, J., Shiroishi, T., and Barna, M. (2011). Ribosome-mediated specificity in Hox mRNA translation and vertebrate tissue patterning. Cell **145:** 383–397.

Kwon, H.K., Yokoyama, R., and Nishitani, K. (2005). A proteomic approach to apoplastic proteins involved in cell wall regeneration in protoplasts of *Arabidopsis* suspension-cultured cells. Plant Cell Physiol. **46:** 843–857.

Latrasse, D., et al. (2011). Control of flowering and cell fate by LIF2, an RNA binding partner of the polycomb complex component LHP1. PLoS ONE **6:** e16592.

Law, S.R., Narsai, R., Taylor, N.L., Delannoy, E., Carrie, C., Giraud, E., Millar, A.H., Small, I., and Whelan, J. (2012). Nucleotide and RNA metabolism prime translational initiation in the earliest events of mitochondrial biogenesis during *Arabidopsis* germination. Plant Physiol. **158:** 1610–1627.

Lee, J., Sayed, N., Hunter, A., Au, K.F., Wong, W.H., Mocarski, E.S., Pera, R.R., Yakubov, E., and Cooke, J.P. (2012). Activation of innate immunity is required for efficient nuclear reprogramming. Cell **151:** 547–558.

López-Bucio, J., Hernández-Abreu, E., Sánchez-Calderón, L., Pérez-Torres, A., Rampey, R.A., Bartel, B., and Herrera-Estrella, L. (2005). An auxin transport independent pathway is involved in phosphate stress-induced root architectural alterations in *Arabidopsis*. Identification of BIG as a mediator of auxin in pericycle cell activation. Plant Physiol. **137:** 681–691.

Lu, T., Yang, Y., Yao, B., Liu, S., Zhou, Y., and Zhang, C. (2012). Template-based structure prediction and classification of transcription factors in *Arabidopsis thaliana*. Protein Sci. **21:** 828–838.

Lurin, C., et al. (2004). Genome-wide analysis of *Arabidopsis* pentatricopeptide repeat proteins reveals their essential role in organelle biogenesis. Plant Cell **16:** 2089–2103.

Mallory, A., and Vaucheret, H. (2010). Form, function, and regulation of ARGONAUTE proteins. Plant Cell **22:** 3879–3889.

Maréchal, A., Parent, J.S., Sabar, M., Véronneau-Lafortune, F., Abou-Rached, C., and Brisson, N. (2008). Overexpression of mtDNA-associated AtWhy2 compromises mitochondrial function. BMC Plant Biol. **8:** 42.

Masson, J., and Paszkowski, J. (1992). The culture response of *Arabidopsis thaliana* protoplasts is determined by the growth-conditions of donor plants. Plant J. **2:** 829–833.

Matsubayashi, Y., Ogawa, M., Morita, A., and Sakagami, Y. (2002). An LRR receptor kinase involved in perception of a peptide plant hormone, phytosulfokine. Science **296:** 1470–1472.

May, M.J., and Leaver, C.J. (1993). Oxidative stimulation of glutathione synthesis in *Arabidopsis thaliana* suspension cultures. Plant Physiol. **103:** 621–627.

Merkwirth, C., and Langer, T. (2009). Prohibitin function within mitochondria: Essential roles for cell proliferation and cristae morphogenesis. Biochim. Biophys. Acta **1793:** 27–32.

Mitsuda, N., and Ohme-Takagi, M. (2009). Functional analysis of transcription factors in *Arabidopsis*. Plant Cell Physiol. **50:** 1232–1248.

Morel, G., and Wetmore, R.H. (1951). Fern callus tissue culture. Am. J. Bot. **38:** 141–143.

Nakashima, K., Kiyosue, T., Yamaguchi-Shinozaki, K., and Shinozaki, K. (1997). A nuclear gene, erd1, encoding a chloroplast-targeted Clp protease regulatory subunit homolog is not only induced by water stress but also developmentally up-regulated during senescence in *Arabidopsis thaliana*. Plant J. **12:** 851–861.

Nitsch, J.P., and Oyama, K. (1971). Obtention de plantes à partir de protoplastes haploïdes cultivés in vitro. C. R. Acad. Sci. Paris **273:** 801–804.

Parizot, B., De Rybel, B., and Beeckman, T. (2010). VisuaLRTC: A new view on lateral root initiation by combining specific transcriptome data sets. Plant Physiol. **153:** 34–40.

Parsons, H.T., et al. (2012). Isolation and proteomic characterization of the *Arabidopsis* Golgi defines functional and novel components involved in plant cell wall biosynthesis. Plant Physiol. **159:** 12–26.

Perrin, R., Lange, H., Grienenberger, J.M., and Gagliardi, D. (2004). AtmtPNPase is required for multiple aspects of the 18S rRNA

metabolism in *Arabidopsis thaliana* mitochondria. Nucleic Acids Res. **32:** 5174–5182.

Pontvianne, F., et al. (2010). Nucleolin is required for DNA methylation state and the expression of rRNA gene variants in *Arabidopsis thaliana*. PLoS Genet. **6:** e1001225.

Provart, N., and Zhu, T. (2003). A browser-based functional classification SuperViewer for *Arabidopsis* genomics. Currents Comp. Mol. Biol. **271:** 2.

Reddien, P.W., Bermange, A.L., Murfitt, K.J., Jennings, J.R., and Sánchez Alvarado, A. (2005). Identification of genes needed for regeneration, stem cell function, and tissue homeostasis by systematic gene perturbation in *planaria*. Dev. Cell **8:** 635–649.

Romera-Branchat, M., Ripoll, J.J., Yanofsky, M.F., and Pelaz, S. (September 4, 2012). The WOX13 homeobox gene promotes replum formation in the *Arabidopsis thaliana* fruit. Plant J. http://dx.doi.org/.

Saeed, A.I., et al. (2003). TM4: A free, open-source system for microarray data management and analysis. Biotechniques **34:** 374–378.

Sampedro, J., and Cosgrove, D.J. (2005). The expansin superfamily. Genome Biol. **6:** 242.

Schmitz-Linneweber, C., and Small, I. (2008). Pentatricopeptide repeat proteins: A socket set for organelle gene expression. Trends Plant Sci. **13:** 663–670.

Sena, G., and Birnbaum, K.D. (2010). Built to rebuild: in search of organizing principles in plant regeneration. Curr. Opin. Genet. Dev. **20:** 460–465.

Shi, D.Q., Liu, J., Xiang, Y.H., Ye, D., Sundaresan, V., and Yang, W.C. (2005). SLOW WALKER1, essential for gametogenesis in *Arabidopsis*, encodes a WD40 protein involved in 18S ribosomal RNA biogenesis. Plant Cell **17:** 2340–2354.

Skoog, F., and Miller, C.O. (1957). Chemical regulation of growth and organ formation in plant tissues cultured in vitro. Symp. Soc. Exp. Biol. **11:** 118–130.

Solana, J., Kao, D., Mihaylova, Y., Jaber-Hijazi, F., Malla, S., Wilson, R., and Aboobaker, A. (2012). Defining the molecular profile of planarian pluripotent stem cells using a combinatorial RNAseq, RNA interference and irradiation approach. Genome Biol. **13:** R19.

Sugimoto, K., Gordon, S.P., and Meyerowitz, E.M. (2011). Regeneration in plants and animals: Dedifferentiation, transdifferentiation, or just differentiation? Trends Cell Biol. **21:** 212–218.

Sugimoto, K., Jiao, Y., and Meyerowitz, E.M. (2010). *Arabidopsis* regeneration from multiple tissues occurs via a root development pathway. Dev. Cell **18:** 463–471.

Szymanski, D.B., and Cosgrove, D.J. (2009). Dynamic coordination of cytoskeletal and cell wall systems during plant cell morphogenesis. Curr. Biol. **19:** R800–R811.

Takahashi, K., and Yamanaka, S. (2006). Induction of pluripotent stem cells from mouse embryonic and adult fibroblast cultures by defined factors. Cell **126:** 663–676.

Takebe, I., Labib, G., and Melchers, G. (1971). Regeneration of whole plants from isolated mesophyll protoplasts of tobacco. Naturwiss. **58:** 318–320.

Talbert, P.B., et al. (2012). A unified phylogeny-based nomenclature for histone variants. Epigenetics Chromatin **5:** 7.

Tessadori, F., Chupeau, M.C., Chupeau, Y., Knip, M., Germann, S., van Driel, R., Fransz, P., and Gaudin, V. (2007). Large-scale dissociation and sequential reassembly of pericentric heterochromatin in dedifferentiated *Arabidopsis* cells. J. Cell Sci. **120:** 1200–1208.

van der Graaff, E., Laux, T., and Rensing, S.A. (2009). The WUS homeobox-containing (WOX) protein family. Genome Biol. **10:** 248.

Vanholme, B., Grunewald, W., Bateman, A., Kohchi, T., and Gheysen, G. (2007). The tify family previously known as ZIM. Trends Plant Sci. **12:** 239–244.

Vanneste, S., et al. (2005). Cell cycle progression in the pericycle is not sufficient for SOLITARY ROOT/IAA14-mediated lateral root initiation in *Arabidopsis thaliana*. Plant Cell **17:** 3035–3050.

Vasil, I.K. (2008). A history of plant biotechnology: From the Cell Theory of Schleiden and Schwann to biotech crops. Plant Cell Rep. **27:** 1423–1440.

Walker, K.L., Muller, S., Moss, D., Ehrhardt, D.W., and Smith, L.G. (2007). *Arabidopsis* TANGLED identifies the division plane throughout mitosis and cytokinesis. Curr. Biol. **17:** 1827–1836.

Widholm, J.M. (1972). The use of fluorescein diacetate and phenosafranine for determining viability of cultured plant cells. Stain Technol. **47:** 189–194.

Xiao, L., Zhang, L., Yang, G., Zhu, H., and He, Y. (2012). Transcriptome of protoplasts reprogrammed into stem cells in *Physcomitrella patens*. PLoS ONE **7:** e35961.

Yadav, R.K., Girke, T., Pasala, S., Xie, M., and Reddy, G.V. (2009). Gene expression map of the *Arabidopsis* shoot apical meristem stem cell niche. Proc. Natl. Acad. Sci. USA **106:** 4941–4946.

Yang, X., Tu, L., Zhu, L., Fu, L., Min, L., and Zhang, X. (2008). Expression profile analysis of genes involved in cell wall regeneration during protoplast culture in cotton by suppression subtractive hybridization and macroarray. J. Exp. Bot. **59:** 3661–3674.

Yoo, S.D., Cho, Y.H., and Sheen, J. (2007). *Arabidopsis* mesophyll protoplasts: A versatile cell system for transient gene expression analysis. Nat. Protoc. **2:** 1565–1572.

Zelcer, A., and Galun, E. (1976). Culture of newly isolated tobacco protoplasts: Precursor incorporation into protein, RNA and DNA. Plant Sci. Lett. **7:** 331–336.

Zhai, Z., Sooksa-nguan, T., and Vatamaniuk, O.K. (2009). Establishing RNA interference as a reverse-genetic approach for gene functional analysis in protoplasts. Plant Physiol. **149:** 642–652.

Zhao, J., Morozova, N., Williams, L., Libs, L., Avivi, Y., and Grafi, G. (2001). Two phases of chromatin decondensation during dedifferentiation of plant cells: Distinction between competence for cell fate switch and a commitment for S phase. J. Biol. Chem. **276:** 22772–22778.

Zhao, X.Y., Su, Y.H., Zhang, C.L., Wang, L., Li, X.G., and Zhang, X.S. (2013). Differences in capacities of in vitro organ regeneration between two *Arabidopsis* ecotypes Wassilewskija and Columbia. Plant Cell Tissue Organ Cult. **112:** 65–74.

Zhang, J., et al. (2011). UCP2 regulates energy metabolism and differentiation potential of human pluripotent stem cells. EMBO J. **30:** 4860–4873.

Zhang, X., Germann, S., Blus, B.J., Khorasanizadeh, S., Gaudin, V., and Jacobsen, S.E. (2007). The *Arabidopsis* LHP1 protein colocalizes with histone H3 Lys27 trimethylation. Nat. Struct. Mol. Biol. **14:** 869–871.

Zhou, W., Choi, M., Margineantu, D., Margaretha, L., Hesson, J., Cavanaugh, C., Blau, C.A., Horwitz, M.S., Hockenbery, D., Ware, C., and Ruohola-Baker, H. (2012). HIF1α induced switch from bivalent to exclusively glycolytic metabolism during ESC-to-EpiSC/hESC transition. EMBO J. **31:** 2103–2116.

Zipori, D. (2004). The nature of stem cells: State rather than entity. Nat. Rev. Genet. **5:** 873–878.

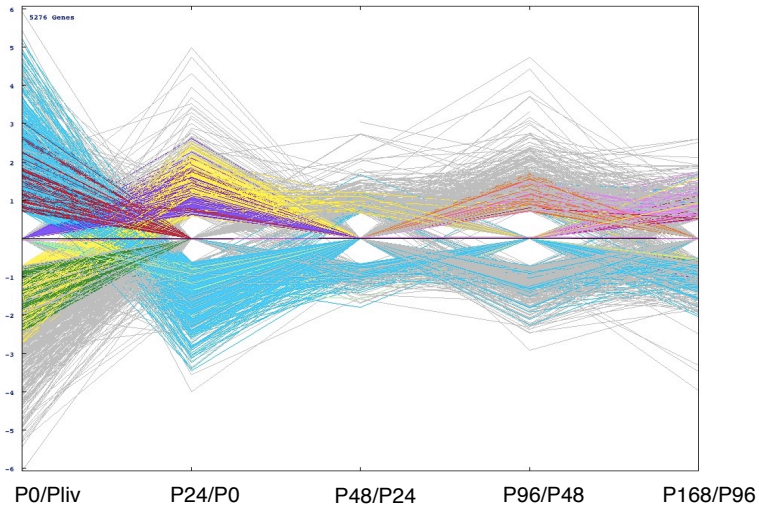

Supplemental Figure 1. Clustering of the transcript profiles.
Expression profiles of the 5276 DE5 genes. Grey represents genes outside of the eight main clusters, and each color represents one of the eight clusters.

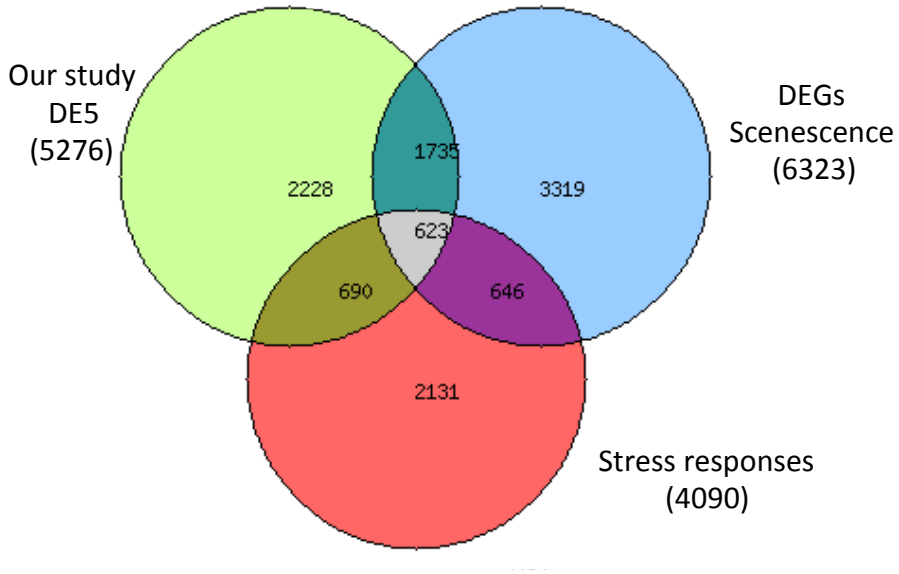

Supplemental Figure 2. Venn diagram showing the distribution of DE5 genes isolated in our study and known to be expressed during senescence and to be involved in stress responses. The numbers in parentheses represent the number of genes in each group. The DEGs expressed during senescence were previously reported (Breeze et al., 2011), as were those involved in stress responses (GO: 0006950).

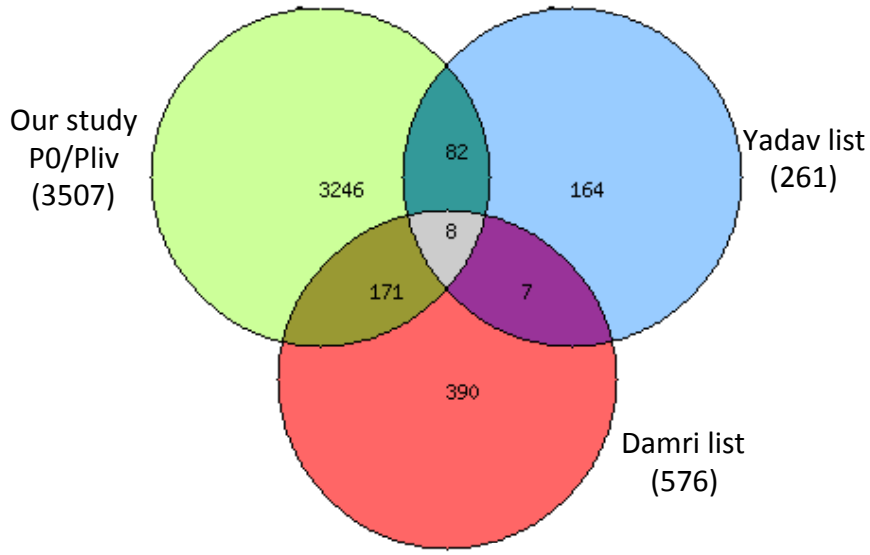

Supplemental Figure 3. Venn diagram showing common genes deregulated in protoplast transciptomes established in our study and in two previous studies. Yadav list: genes deregulated in protoplasts (Yadav et al., 2009). Damri list: genes associated with meristem protoplasting (Damri et al., 2009)

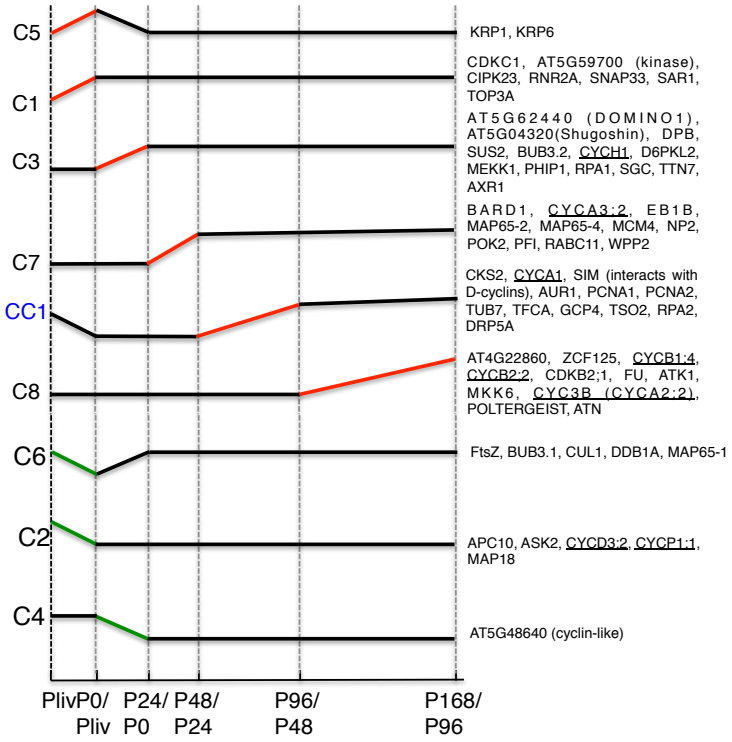

Supplemental Figure 4. The expression of *A. thaliana* cell cycle genes at various time points during protoplast culture.
Schematic representation of the eight gene clusters and cluster CC1, showing waves of activation (red) and repression (green). A selection of genes involved in the cell division cycle is give for each cluster. Cyclin genes are underlined.

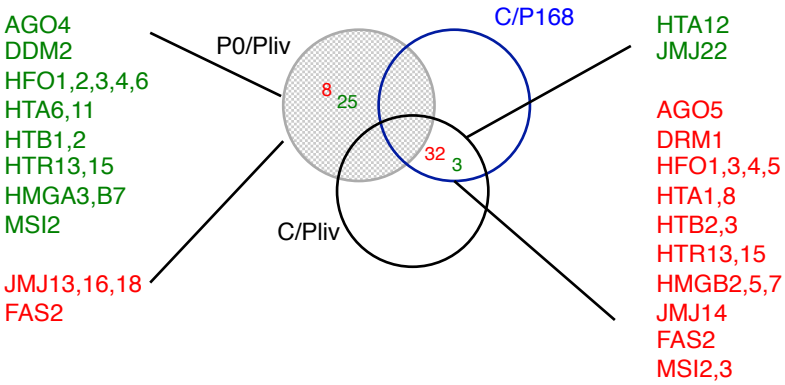

Supplemental Figure 5. Venn diagram highlighting genes specific to cell suspension (common in C/P168 and C/Pliv) or to the protoplast stage (only deregulated in P0/Pliv). A selection of genes downregulated (green) or upregulated (red) and associated with chromatin regulation are indicated for each group.

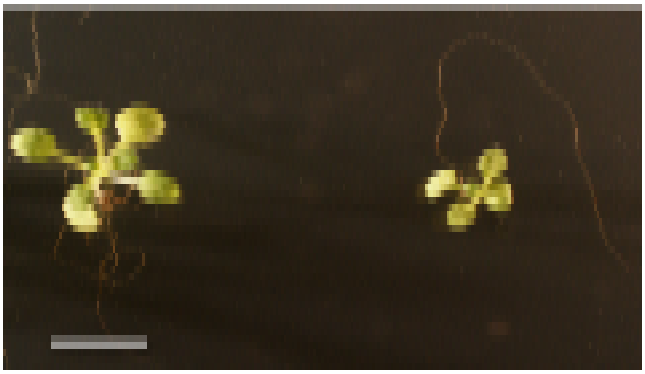

Supplemental Figure 6. Phenotype of the *alf4-1* mutant.
Left, a three-week-old wild-type col-0 seedling. Right, a three-week-old *alf4-1* homozygous plantlet. Note the reduction in the number of lateral roots in the mutant compared to the wild-type plantlet. Bar = 1 cm.

	GM[a]	MGG[b]	PIM[c]	CIM1[d]	CIM2[d]	SIM[e] Col-0	SIM[e] Ws	PDM[f]
Macrosalts								
KNO_3	950	250	505	505	1010	1010	1010	950
NH_4NO_3	825		160	400	800	0	800	825
$CaCl_2$, $2H_2O$	220	15	440	440	440	220	220	220
$MgSO_4$, $7H_2O$	185	25	370	370	370	185	185	185
KH_2PO_4	85		170	170	170	85	85	85
$(NH4)_2SO_4$		13.4						
NaH_2PO_4		15						
Microelements								
Fe Citrate NH_4[g]	50		30	30	30	50	50	50
KI	0.4	0.75	0.01	0.01	0.01	0.8	0.8	0.01
H_3BO_3	1.5	3	1	1	1	3	3	1
$MnCl_2$, $4H_2O$	15					30	30	
$MnSO_4$, $4H_2O$		10	0.1	0.1	0.1			0.1
$ZnSO_4$, $7H_2O$	6	2	1	1	1	12	12	1
Na_2MoO_4, $2H_2O$	0.45	0.25				0.9	0.9	
CuSO4, $5H_2O$	0.045	0.025	0.03	0.03	0.03	0.09	0.09	0.03
$CoCl_2$, $6H_2O$	0.045	0.025				0.09	0.09	
$AlCl_3$			0.03	0.03	0.03			0.03
$NiCl_2$, $6H_2O$			0.03	0.03	0.03			0.03
Vitamins								
Inositol	100	100	100	100	100	100	100	100
Panthotenate Ca	1	1	1	1	1	1	1	1
Biotin	0.01	0.01	0.01	0.01	0.01	0.01	0.01	0.01
Niacin	1	1	1	1	1	1	1	1
Pyridoxin	1	1	1	1	1	1	1	1
Thiamin	1	1	1	1	1	1	1	1
Folic Acid			0.2					
Other constituants								
Glucose		45 000	40 000	0				
Sucrose	10 000		0	30 000	20 000	20 000	20 000	10 000
Mannitol			60 000	70 000	60 000	40 000	40 000	
Glycine		25 000						
2, 4-D			1	0	0	0	0	
Thidiazuron (TZ)			0.022	0.11	0.22			
Indole-3-butyric acid (IBA)						0,1	0,1	
Meta-topolin						0.2	0.2	
MES	700	700	700	700	700	700	700	700
Bromocresol purple (BCP)[h]	8	8	8	8	8	8	8	8
Vitro Agar	6 000					6 000	6 000	4 000
Onozuka R10		1 000						
Macerozyme		300						
Driselase		400						
pH of fresh medium	5.6	5.6	5.6	5.6	5.6	5.6	5.6	5.6

[a]Germination medium. Half macrosalts of Murashige and Skoog (1962). Vitamin composition based on Morel and Wetmore (1951).
[b]Maceration-glycine-glucose medium. One tenth of macrosalts. Microsalts based on Gamborg et al. (1968).
[c]Protoplast-induction medium. Microsalts based on Heller (1953).
[d]Colony-induction medium.
[e]Shoot-induction medium.
[f]Plant development medium.
[g]FeCitrate NH_4 is less toxic than FeEDTA, solutions at pH 5.6 make easy to test ranges.
[h]BCP is a convenient, non-toxic pH indicator (Roscoe and Bell, 1981).

Supplemental Table 1. Media compositions for *A. thaliana* protoplast culture (mg/L).

		RT-qPCR (normalized delta Ct)				Log_2 ratio (microarray data)			
AGI	Name	P0/Pliv	P24/P0	P48/P24	P96/P48	P0/Pliv	P24/P0	P48/P24	P96/P48
AT2G43000	ANAC042/NAM2	5.16	-1.82			3.41	-1.71	0,00	0,00
AT1G02220	ANAC003/NAM1	4.23	-2.16			2.80	-1.04	0,00	0,00
AT3G19150	KPR6/ICK6	3.09	-0.73			1.02	-0.65	0,00	0,00
AT2G23430	KPR1/ICK1	1.38	-2.06	1,11		1.01	-1.46	0,00	0,00
AT5G55280	FtsZ	-1.965	1.49	0,53	-2.16	-1.93	1.79	0,00	0,00
AT1G12980	ESR1			2,59	0.75	0,00	0,00	0.76	2.52
AT2G22490	CYCD2-1		0.61	0,63	-1.63	0,00	0.59	0,00	0,00
AT5G57900	SKIP1/ASK1	2.46	-1.12		-1.01	2.14	-0.89	0,00	0,00

Supplemental Table 2. Validation of microarray data. Expression profiles of a set of genes as determined by RT-qPCR in comparison with microarray hybridization data.

GO BAR	C1			C2			C3			C4			C5			C6			C7			C8		
Biological process	NF		p-Value	NF		p-Value	NF		p-Value	NF		p-Value	NF		p-Value	NF		p-Value	NF		p-Value	NF		p-Value
Cell organization and biogenesis	1.28	± 0.116	2.070e-03	**1.73**	**± 0.128**	**7.549e-12**	2.34	± 0.168	6.114e-24	0.94	± 0.161	2.070e-03	1.05	± 0.086	0.035	2.37	± 0.181	9.565e-21	1.25	± 0.196	0.044	1.76	± 0.232	9.311e-05
Developmental processes	1.17	± 0.121	0.011	1.44	± 0.091	1.451e-06	1.72	± 0.135	4.187e-10	0.7	± 0.133	0.011	0.86	± 0.081	0.011	1.55	± 0.153	4.761e-06	1.23	± 0.203	0.041	**2.03**	**± 0.21**	**7.842e-08**
DNA or RNA metabolism	0.78	± 0.207	0.062	0.42	± 0.134	7.328e-04	**2.69**	**± 0.368**	**6.485e-10**	0.65	± 0.238	0.062	0.48	± 0.108	6.666e-04	1.04	± 0.268	0.104	**2.51**	**± 0.667**	**9.766e-04**	1.65	± 0.486	0.035
Electron transport or energy pathways	**2.22**	**± 0.388**	**1.567e-05**	**3.47**	**± 0.422**	**2.544e-17**	**2.36**	**± 0.426**	**6.340e-06**	0.73	± 0.345	1.567e-05	0.91	± 0.186	0.084	**2.4**	**± 0.464**	**2.562e-05**	0.23	± 0.205	0.062	1.6	± 0.549	0.064
Other biological processes	1.95	± 0.129	7.811e-16	1.33	± 0.106	2.133e-04	1.37	± 0.136	3.038e-04	1.36	± 0.173	7.811e-16	2.55	± 0.132	1.371e-53	1.26	± 0.122	6.571e-03	1.56	± 0.217	2.573e-03	**2.07**	**± 0.232**	**1.165e-07**
Other cellular processes	1.32	± 0.042	9.131e-16	1.2	± 0.036	6.936e-09	1.43	± 0.037	1.226e-24	1.03	± 0.065	9.131e-16	1.26	± 0.035	3.480e-16	1.62	± 0.042	5.111e-42	1.18	± 0.07	3.669e-03	1.17	± 0.068	3.069e-03
Other metabolic processes	1.32	± 0.042	2.676e-14	1.21	± 0.04	8.315e-09	1.39	± 0.042	9.322e-19	0.96	± 0.064	2.676e-14	1.3	± 0.038	5.984e-19	1.62	± 0.048	1.415e-36	1.07	± 0.079	0.039	1.14	± 0.069	8.716e-03
Protein metabolism	1.3	± 0.101	8.478e-05	0.94	± 0.079	0.031	1.72	± 0.105	1.012e-14	0.59	± 0.091	8.478e-05	0.91	± 0.066	0.018	**2.41**	**± 0.124**	**5.065e-38**	0.94	± 0.16	0.075	1.18	± 0.156	0.032
Response to abiotic or biotic stimulus	**2.01**	**± 0.14**	**9.125e-19**	1.49	± 0.113	1.959e-07	1.58	± 0.14	2.209e-07	1.11	± 0.143	9.125e-19	**2.62**	**± 0.132**	**3.730e-62**	1.5	± 0.15	2.587e-05	0.71	± 0.169	0.033	1.42	± 0.203	5.933e-03
Response to stress	1.96	± 0.143	3.006e-19	1.04	± 0.087	0.037	1.41	± 0.122	2.744e-05	1.21	± 0.156	3.006e-19	**2.68**	**± 0.12**	**2.843e-74**	1.2	± 0.13	0.011	0.76	± 0.167	0.042	0.94	± 0.169	0.078
Signal transduction	1.73	± 0.192	1.904e-06	0.92	± 0.137	0.052	0.87	± 0.145	0.051	0.75	± 0.198	1.904e-06	2.43	± 0.17	2.785e-25	0.64	± 0.125	7.422e-03	**1.57**	**± 0.319**	**0.015**	1.52	± 0.298	0.013
Transcription, DNA-dependent	1.09	± 0.139	0.041	1.17	± 0.117	0.017	1.3	± 0.151	4.539e-03	1.11	± 0.214	0.041	1.11	± 0.112	0.025	0.92	± 0.137	0.060	0.75	± 0.204	0.068	1.95	± 0.27	3.125e-05
Transport	1.91	± 0.125	7.902e-15	1.25	± 0.11	1.773e-03	1.86	± 0.154	1.600e-12	1.43	± 0.178	7.902e-15	1.59	± 0.1	4.632e-11	0.94	± 0.117	0.054	1.13	± 0.235	0.072	1.34	± 0.194	0.016
Unknown biological processes	0.65	± 0.049	2.088e-10	0.85	± 0.047	6.629e-04	0.73	± 0.057	1.479e-06	1.11	± 0.085	2.088e-10	0.82	± 0.042	2.433e-05	0.51	± 0.058	5.482e-15	0.86	± 0.104	0.031	0.82	± 0.089	0.013
Molecular function																								
DNA or RNA binding	0.78	± 0.104	7.310e-03	0.79	± 0.098	5.277e-03	1.25	± 0.135	5.299e-03	0.89	± 0.164	0.063	0.72	± 0.079	2.845e-04	1.36	± 0.155	1.287e-03	0.49	± 0.14	3.469e-03	0.98	± 0.19	0.087
Hydrolase activity	1	± 0.1	0.053	1.11	± 0.11	0.026	1.39	± 0.13	4.167e-04	0.81	± 0.15	0.044	0.93	± 0.089	0.034	0.78	± 0.123	0.017	1.17	± 0.24	0.067	**1.6**	**± 0.253**	**1.271e-03**
Kinase activity	**1.98**	**± 0.253**	**4.974e-07**	1.07	± 0.169	0.061	0.85	± 0.173	0.066	0.67	± 0.166	0.057	0.75	± 0.132	0.015	0.8	± 0.22	0.062	1.22	± 0.361	0.106	**1.74**	**± 0.416**	**9.507e-03**
Nucleic acid binding	0.63	± 0.128	5.440e-03	0.32	± 0.088	1.369e-07	1.78	± 0.236	1.418e-05	0.31	± 0.143	8.878e-04	0.31	± 0.068	3.900e-09	0.72	± 0.181	0.030				0.34	± 0.154	6.322e-03
Nucleotide binding	**1.63**	**± 0.15**	**2.876e-08**	0.9	± 0.09	0.032	**2.05**	**± 0.172**	**2.485e-16**	0.56	± 0.125	1.539e-03	0.73	± 0.079	3.903e-04	1.32	± 0.129	2.689e-03	0.93	± 0.186	0.092	1.35	± 0.219	0.015
Other binding	1.36	± 0.068	3.069e-07	0.87	± 0.063	5.431e-03	1.09	± 0.097	0.019	0.85	± 0.096	0.022	1.03	± 0.067	0.027	0.97	± 0.073	0.043	1.12	± 0.143	0.045	1.17	± 0.136	0.025
Other enzyme activity	1.5	± 0.114	1.416e-06	1.28	± 0.104	7.363e-04	0.99	± 0.109	0.052	1.27	± 0.184	0.015	**1.52**	**± 0.107**	**1.617e-09**	1.17	± 0.134	0.021	0.9	± 0.189	0.084	0.83	± 0.184	0.058
Other molecular functions	1.12	± 0.205	0.064	1.21	± 0.18	0.033	0.75	± 0.154	0.044	0.93	± 0.248	0.119	1.38	± 0.197	3.996e-03	0.48	± 0.156	5.160e-03	**1.8**	**± 0.445**	**0.016**	1.27	± 0.365	0.089
Protein binding	1.58	± 0.176	9.831e-06	1.04	± 0.13	0.049	1.54	± 0.167	4.975e-05	1.21	± 0.219	0.042	1.37	± 0.125	1.346e-04	1.64	± 0.183	2.528e-05	1.13	± 0.248	0.089	1.56	± 0.242	5.411e-03
Receptor binding or activity	1.09	± 0.511	0.195	1.12	± 0.462	0.173	1.2	± 0.635	0.185	**1.73**	**± 1.032**	**0.154**	**1.63**	**± 0.571**	**0.051**	0.73	± 0.47	0.244	0.94	± 0.889	0.369	0.79	± 0.668	0.359
Structural molecule activity	0.43	± 0.204	0.017	1.29	± 0.322	0.054	**2.22**	**± 0.47**	**2.124e-04**	0.73	± 0.331	0.160	0.46	± 0.167	5.599e-03	**14.13**	**± 1.039**	**6.391e-105**	0.9	± 0.462	0.223	0.25	± 0.196	0.074
Transcription factor activity	1.11	± 0.168	0.052	1.14	± 0.162	0.037	0.59	± 0.14	3.764e-03	1.2	± 0.269	0.065	1.41	± 0.157	5.162e-04	0.3	± 0.1	1.366e-05	0.69	± 0.253	0.086	1.9	± 0.347	1.279e-03
Transferase activity	1.53	± 0.143	7.987e-06	1.08	± 0.104	0.036	1.32	± 0.149	2.274e-03	0.65	± 0.126	0.010	0.96	± 0.092	0.043	1.08	± 0.147	0.050	1.17	± 0.254	0.068	1.12	± 0.223	0.071
Transporter activity	1.46	± 0.224	4.608e-03	0.89	± 0.175	0.061	1.19	± 0.239	0.048	1.34	± 0.325	0.049	0.89	± 0.156	0.053	0.49	± 0.159	4.918e-03	1.03	± 0.364	0.143	1.51	± 0.356	0.036
Unknown molecular functions	0.65	± 0.05	6.306e-10	0.98	± 0.05	0.031	0.56	± 0.046	3.402e-13	1.02	± 0.092	0.050	0.91	± 0.047	5.972e-03	0.5	± 0.056	1.572e-14	0.96	± 0.121	0.064	0.84	± 0.095	0.019
Cellular component																								
Cell wall	1.65	± 0.335	8.393e-03	1.48	± 0.302	0.016	1.99	± 0.413	8.420e-04	0.82	± 0.314	0.161	0.67	± 0.192	0.034	4.19	± 0.631	2.225e-14	0.81	0.366	0.211	**2.04**	**± 0.651**	**0.020**
Chloroplast	0.99	± 0.122	0.048	2.5	± 0.128	5.871e-47	1.56	± 0.133	1.598e-07	1.3	± 0.178	8.367e-03	0.98	± 0.094	0.039	2.46	± 0.154	5.339e-28	0.54	0.139	4.001e-03	0.56	± 0.111	2.612e-03
Cytosol	**2.17**	**± 0.229**	**9.015e-11**	0.84	± 0.14	0.038	**3.08**	**± 0.273**	**6.828e-24**	0.6	± 0.178	0.025	1.45	± 0.142	2.194e-04	**6.44**	**± 0.39**	**6.687e-92**	**2.17**	**0.402**	**3.062e-04**	1.4	± 0.276	0.039
ER	**2.08**	**± 0.433**	**2.943e-04**	1.09	± 0.267	0.096	2.2	± 0.466	1.802e-04	**1.75**	**± 0.575**	**0.033**	1.7	± 0.297	1.383e-03	1.99	± 0.437	2.579e-03	1.72	0.726	0.076	0.24	± 0.172	0.063
Extracellular	0.58	± 0.106	8.849e-05	1.3	± 0.13	1.387e-03	0.41	± 0.089	2.245e-07	0.93	± 0.156	0.077	0.69	± 0.085	2.534e-04	0.82	± 0.119	0.030	1.18	0.236	0.071	1.38	± 0.254	0.018
Golgi apparatus	1.41	± 0.274	0.017	0.47	± 0.151	1.835e-03	1.21	± 0.24	0.060	1.32	± 0.408	0.074	1.18	± 0.192	0.044	1.19	± 0.292	0.077	**2.53**	**0.669**	**8.957e-04**	1.06	± 0.4	0.150
Mitochondria	1.09	± 0.117	0.033	0.68	± 0.084	1.787e-04	1.69	± 0.14	3.607e-09	0.82	± 0.153	0.041	0.98	± 0.088	0.041	1.04	± 0.118	0.053	0.65	0.172	0.021	0.54	± 0.141	3.274e-03
Nucleus	1.21	± 0.061	4.214e-05	0.77	± 0.047	2.582e-06	1.31	± 0.06	5.477e-08	0.98	± 0.083	0.050	1	± 0.046	0.029	1.05	± 0.083	0.028	0.92	0.106	0.053	1.17	± 0.108	0.012
Other cellular components	1.66	± 0.251	8.678e-04	1.28	± 0.208	0.023	1.97	± 0.347	2.026e-05	0.94	± 0.337	0.126	1.07	± 0.157	0.063	5.02	± 0.485	3.730e-35	1.24	0.459	0.120	1.95	± 0.443	6.048e-03
Other cytoplasmic components	1.32	± 0.093	7.975e-06	1.41	± 0.07	2.809e-09	1.58	± 0.096	3.589e-12	1.25	± 0.136	5.118e-03	1.38	± 0.064	6.986e-10	2.69	± 0.107	2.927e-64	1.29	0.145	9.747e-03	1.08	± 0.127	0.054
Other intracellular components	1.14	± 0.084	0.011	1.62	± 0.088	1.137e-14	2.01	± 0.116	8.426e-25	1.13	± 0.157	0.034	0.93	± 0.069	0.023	3.33	± 0.131	6.523e-90	1.12	0.141	0.057	0.85	± 0.127	0.048
Other membranes	1.15	± 0.109	0.015	1.52	± 0.106	4.424e-08	1.46	± 0.143	1.123e-05	1.09	± 0.152	0.055	0.92	± 0.081	0.027	2.03	± 0.158	4.914e-15	1.4	0.207	0.011	1.06	± 0.17	0.075
Plasma membrane	1.84	± 0.13	3.469e-12	1.11	± 0.1	0.025	1.21	± 0.134	0.010	1.18	± 0.177	0.039	1.24	± 0.092	1.515e-03	1.75	± 0.147	4.618e-08	1.88	0.291	5.674e-05	**1.92**	**± 0.242**	**6.558e-06**
Plastid	0.8	± 0.158	0.045	**3.66**	**± 0.245**	**3.145e-38**	1.53	± 0.244	2.038e-03	**1.61**	**± 0.352**	**8.541e-03**	0.92	± 0.154	0.057	3.53	± 0.382	4.125e-22	0.48	0.227	0.047	0.5	± 0.207	0.037
Ribosome	0.39	± 0.169	0.017	0.97	± 0.296	0.116	**2.62**	**± 0.53**	**1.315e-05**	0.2	± 0.159	0.039	0.39	± 0.154	3.779e-03	**15.76**	**± 1.165**	**3.011e-109**	1.02	0.487	0.226			
Unknown cellular components	0.45	0.056	3.539e-18	0.55	0.049	4.268e-15	0.43	0.049	3.974e-18	0.6	0.078	9.257e-06	0.59	0.051	4.773e-15	0.28	0.048	3.926e-25	0.85	0.129	0.038	0.66	0.102	7.641e-04

Supplemental Table 3. Complete GO descriptions of the eight main clusters identified in this study.

AGI	Name	Function
AT1G77920		bZIP transcription factor family
AT2G16720	MYB DOMAIN PROTEIN 7	
AT2G26150	HEAT SHOCK FACTOR A2	
AT3G24500	MULTIPROTEIN BRIDGING FACTOR 1C	Conserved transcriptional coactivator. May serve as a bridging factor between a bZIP factor and TBP
AT4G36710	HAM4	GRAS transcription factor family
AT4G36990	HEAT SHOCK FACTOR 4	
AT5G29000	PHR1-LIKE 1 (PHL1)	Homeodomain-like superfamily protein
AT5G47370	HAT2	Homeobox-leucine zipper genes induced by auxin

Supplemental Table 4 List of DEGs common to our study (P0/Pliv) and two previous studies (Damri et al., 2009 and Yadav et al., 2009).

AGI	Name
AT1G19850	MONOPTEROS (MP)
AT1G21460	SWEET1
AT1G64670	BODYGUARD1 (BDG1)
AT1G73590	PIN-FORMED 1 (PIN1)
AT1G75820	CLAVATA 1 (CLV1)
AT1G76110	HMG
AT2G34710	PHABULOSA (PHB)
AT2G42840	PROTODERMAL FACTOR 1 (PDF1)
AT3G53980	Lipid transfer protein
AT3G59420	CRINKLY4 (CR4)
AT4G04890	PROTODERMAL FACTOR 2 (PDF2)
AT4G21750	MERISTEM LAYER 1 (ATML1)
AT4G34590	BZIP11
AT4G36930	SPATULA (SPT)
AT4G39480	CYP96A9
AT5G06300	Decarboxylase
AT5G20240	PISTILLATA (PI)
AT5G57390	AINTEGUMENTA-LIKE 5 (AIL5)

Supplemental Table 5. List of DEGs deregulated in DE5 (5276) and present among the 70 genes involved in stem cell formation (Yadav et al., 2009).

AGI	Name	Family	Cluster	References
AT2G26150	HEAT SHOCK FACTOR A2		cluster 5	this study/ Damri/Yadav
AT4G36990	HEAT SHOCK FACTOR 4		cluster 5	this study/ Damri/Yadav
AT1G77920		bZIP transcription factor family	cluster 5	this study/ Damri/Yadav
AT2G16720	MYB DOMAIN PROTEIN 7	Myb transcription factor family	cluster 5	this study/ Damri/Yadav
AT3G24500	MULTIPROTEIN BRIDGING FACTOR 1C	Transcriptional coactivator	cluster 5	this study/ Damri/Yadav
AT4G36710	HAM4	GRAS transcription factor family	cluster 5	this study/ Damri/Yadav
AT5G29000	PHR1-LIKE 1 (PHL1)	Homeodomain-like superfamily protein	cluster 5	this study/ Damri/Yadav
AT5G47370	HAT2	Homeobox-leucine zipper genes induced by auxin	cluster 6	this study/ Damri/Yadav
AT4G17500		ERF family	cluster 5	this study/ Xiao et al., 2012
AT1G74950	TIFY10B	Jasmonate-zim-domain protein	cluster 5	this study/ Xiao et al., 2012
AT1G10170	ATNFXL1	Putative transcriptional repressor	cluster 5	this study/ Xiao et al., 2012
AT5G28770	bZIP63	bZIP transcription factor family		this study/ Xiao et al., 2012

Supplemental Table 6. List of genes deregulated DEG in Pliv/P0 (this work), meristem protoplasts (Yadav et al., 2009), and moss protoplasts (Xiao et al., 2012).

AGI	Function	Alias	PO/ Pliv	P24/ P0	P48/ P24	P96/ P48	P168/ P96	Cluster	Asymetric division	Pericycle differential expression	Auxin response	Cell cycle phase	Cell type
Biosynthesis pathway													
AT5G05730	anthranilate synthase alpha subunit 1		0,86					Cluster 1		P	1,017		
AT1G51780	IAA-leucine resistant (ILR)-like gene 5		0,93		NA			Cluster 1					
AT4G15550	indole-3-acetate beta-D-glucosyltransferase		1,12			NA		Cluster 1		P	6,134		
AT3G44320	nitrilase 3		1,61					Cluster 1	4		-1,385	S	
AT5G38530	tryptophan synthase beta type 2		2,00					Cluster 1			-1,08		
AT4G39950	cytochrome P450, family 79, subfamily B		2,69	-1,73			-1,59	Cluster 5	4	P	-3,243		
AT4G31500	cytochrome P450, family 83, subfamily B			-0,89		-1,10	-1,28	Cluster 5	4	P	-1,208		
AT3G54640	tryptophan synthase alpha chain		2,37	-1,85			-0,55	Cluster 5			1,111		
AT5G54810	tryptophan synthase beta-subunit 1		3,10	-2,11			-0,79	Cluster 5					
AT4G27070	tryptophan synthase beta-subunit 2		2,69		-0,66			Cluster 5					
AT5G55250	IAA carboxylmethyltransferase 1 (IAMT1)					1,64	2,51				1,84		
AT3G44310	nitrilase 1		2,27			-0,77							
AT3G44300	nitrilase 2		3,73	1,00		-0,76							
AT4G24670	tryptophan aminotransferase related 2		-1,05					Cluster 2		X	-1,272		S32|SUC2|APL
AT2G20610	Tyrosine transaminase family protein			-1,04			-0,85	Cluster 4	4		-1,165		
AT2G23170	Auxin-responsive GH3 family protein		0,84	4,31							141,4		CORTEX
AT4G37390	Auxin-responsive GH3 family protein		2,08	3,53			-0,90						
Transporters													
AT1G76530	Auxin efflux carrier family protein		2,27			-1,26	-0,67				-1,01		
AT1G76520	Auxin efflux carrier family protein		2,12	-0,68		-1,04	-0,63	Cluster 5			-1,085		PET111
AT5G54490	pinoid-binding protein 1	PBP1	1,07			0,82	-0,86				24,6	G1	COBL9
AT1G73590	Auxin efflux carrier family protein	PIN1			0,88	1,23	1,12		1		4,973	G2	S4
AT1G77110	Auxin efflux carrier family protein	PIN6					0,58	Cluster 8			1,003		
AT2G34570	PIN domain-like family protein	MEE21		1,38				Cluster 3	9	X	1,528		
AT2G01420	Auxin efflux carrier family protein	PIN4	-1,48		0,91						1,751		
Regulators													
AT2G47770	TSPO(outer membrane tryptophan-rich sensory protein)-related		2,10	-2,16				Cluster 5		P	1,005		
AT5G49980	auxin F-box protein 5	AFB5	-1,07	0,60				Cluster 6			1,013		
AT3G26810	auxin signaling F-box 2	AFB2	-0,71	0,74				Cluster 6		X	-1,478		
Auxin induced genes													
AT5G35735	Auxin-responsive family protein		0,71					Cluster 1			1,167	S	
AT1G51950	indole-3-acetic acid inducible 18	IAA18	1,12					Cluster 1		P	1,67		
AT4G05530	indole-3-butyric acid response 1		1,44					Cluster 1			-1,045		
AT2G45210	SAUR-like auxin-responsive protein family		1,89					Cluster 1		P	1,283		
AT5G53590	SAUR-like auxin-responsive protein family		1,80					Cluster 1					
AT1G59750	auxin response factor 1	ARF1	-1,17					Cluster 2		P	1,162		
AT2G28350	auxin response factor 10	ARF10	-0,91					Cluster 2			-1,132		PET111
AT5G37020	auxin response factor 8	ARF8	-0,97					Cluster 2			-1,502		
AT2G04850	Auxin-responsive family protein		-0,73					Cluster 2			-1,341		S18
AT3G23050	indole-3-acetic acid 7	AXR2, IAA7	-1,27					Cluster 2			1,898		PET111
AT1G17345	SAUR-like auxin-responsive protein family		-0,78					Cluster 2					
AT1G72430	SAUR-like auxin-responsive protein family		-1,03					Cluster 2			-1,424	M	
AT2G21210	SAUR-like auxin-responsive protein family		-2,08					Cluster 2			-1,596		
AT4G00880	SAUR-like auxin-responsive protein family		-1,17					Cluster 2		P	-1,221		SUC2|APL
AT4G34760	SAUR-like auxin-responsive protein family		-2,34				-0,60	Cluster 2			1,914		
AT4G38860	SAUR-like auxin-responsive protein family		-1,11					Cluster 2			1,47		
AT3G02260	auxin transport protein (BIG)	BIG, CRM1, TIR3, LPR1		0,66			0,51	Cluster 3		X	1,047		
AT5G65670	indole-3-acetic acid inducible 9	IAA9		0,70				Cluster 3			1,979		
AT1G80680	SUPPRESSOR OF AUXIN RESISTANCE 3			0,69				Cluster 3			-1,05		S4
AT4G14430	indole-3-butyric acid response 10		1,91	-0,69				Cluster 5	4		1,222		
AT3G60690	SAUR-like auxin-responsive protein family		0,99	-0,69				Cluster 5			-1,095		
AT1G19850	Transcriptional factor B3 family protein / AUX/IAA-related	IAA24, ARF5, MP	2,30	-0,73			0,85	Cluster 5	2		1,593		
AT4G28640	indole-3-acetic acid inducible 11	IAA11	-1,56	2,17				Cluster 6	9		6,599		S18
AT4G32280	indole-3-acetic acid inducible 29	IAA29				0,71		Cluster 7	1		138,6		S18
AT1G30330	auxin response factor 6	ARF6					0,69	Cluster 8		X	-1,215		
AT2G46990	indole-3-acetic acid inducible 20	IAA20				0,88	1,29	Cluster 8	3		2,924		
AT3G07390	auxin-responsive family protein		1,07	1,19	0,86	0,72			5		7,093	S	
AT3G25290	Auxin-responsive family protein		2,03	-1,61		2,17			2		2,538	S	
AT3G15540	indole-3-acetic acid inducible 19	MSG2, IAA19		1,34		2,10			1	P	22,71		
AT1G33410	SUPPRESSOR OF AUXIN RESISTANCE1			0,84		-0,81	0,58			X	1,042		
AT1G15580	indole-3-acetic acid inducible 5	ATAUX2-27, IAA5		0,64		0,74	-0,68		9		180		COBL9
AT3G04730	indoleacetic acid-induced protein 16	IAA16				-1,21	0,84				1,197		
AT3G59900	auxin-regulated gene involved in organ size			-1,19		2,34				P	15,14		S32
AT2G46690	SAUR-like auxin-responsive protein family			-2,12					9		-1,508		
AT2G22670	indoleacetic acid-induced protein 8	IAA8	-2,93	0,99	0,70	1,40	0,83			P	1,142		
AT5G01240	like AUXIN RESISTANT 1		-0,98			1,09	0,65			P	-1,148		RM1000
AT5G60450	auxin response factor 4	ARF4	-0,99			1,09	0,59		5		1,581		SUC2
AT1G56150	SAUR-like auxin-responsive protein family		-1,02		1,39	1,46					1,071		
AT1G56220	Dormancy/auxin associated family protein		-1,05				0,64			P	-1,072		
AT5G43700	AUX/IAA transcriptional regulator family protein	IAA4, ATAUX2-11	-3,48		1,02	1,34					3,548		
AT4G38840	SAUR-like auxin-responsive protein family		-4,40								1,024		
AT5G25890	indole-3-acetic acid inducible 28	IAR2, IAA28	-1,20	-0,71							-1,437		SUC2
AT2G33830	Dormancy/auxin associated family protein		-1,11	-1,00		-0,77			8	P	-1,797		

Supplemental Table 7. Expression profiles of auxin-related genes at various time points in *A. thaliana* protoplast culture.

Clusters	Total	AP2-EREBP	ARF	AUX/IAA	bHLH	bZIP	GRAS	HFS	HB	MADS	MYB related	NAC	Orphan	Tify	WRYKY	Zf-HD
C1	61	5	0	1	2	2	2	0	0	1	8	2	2	0	4	0
C2	65	3	3	1	2	1	1	0	5	4	5	0	3	0	0	2
C3	41	3	0	1	0	1	2	0	0	0	1	0	1	0	1	0
C4	30	6	0	0	1	3	0	0	0	0	3	0	0	0	1	1
C5	109	7	1	0	3	6	1	4	2	1	12	10	1	7	6	0
C6	18	1	0	1	0	0	0	0	2	0	0	0	2	0	1	1
C7	11	1	0	1	0	1	0	0	1	1	0	1	2	0	0	0
C8	30	1	1	1	0	0	1	0	2	2	1	3	0	0	1	1
Others	135	13	1	6	5	6	1	0	10	3	2	6	2	0	10	0
Total	500	40	6	12	13	20	8	4	22	12	32	22	13	7	24	5

Supplemental Table 8. Selected TF families and their distribution in the eight clusters identified in this study.

AGI	Name	Family	Function	P0/Pliv	P24/P0	P48/ P24	P96/ P48	P168/ P96	C/ P168	C/Pliv
AT1G78080	WIND1, related to AP2 4 (RAP2.4)	AP2-EREBP		1,63					-1,64	
AT5G57390	AINTEGUMENTA-LIKE 5 (AIL5)	AP2-EREBP						1,21		1,99
AT1G12980	ENHANCER OF SHOOT REGENERATION 1 (ESR1)	AP2-EREBP				0,76	2,51	1,32	-3,46	0,85
AT1G36060	WIND3	AP2-EREBP		-0,75		0,70	2,43	1,62	-1,61	2,06
AT1G19850	MONOPTEROS (MP)	ARF		2,30	-0,73			0,85	-0,73	1,71
AT4G36930	SPATULA (SPT)	bHLH		0,95						
AT4G34590	G-box binding factor 6 (GBF6)	bZIP			1,02				-0,73	
AT3G54810	BLUE MICROPLYLAR END3 (BME3)	C2C2-GATA			-0,75	0,76		-0,68		
AT5G26930	GATA transcription factor 23	C2C2-GATA					0,97	-0,63		
AT2G27100	SERRATE (SE)	C2H2(Zn)			0,87					NA
AT1G21970	LEAFY COTYLEDON 1(LEC1)	CCAAT						0,69	-1,44	
AT4G38680	COLD SHOCK DOMAIN PROTEIN (CSP2)	CSD		-1,85	1,12					
AT1G61730	DNA-binding storekeeper protein-related	GeBP			1,25					
AT4G17460	HAT1	HB		-1,20			NA			NA
AT4G21750	MERISTEM LAYER 1(ATML1)	HB		-1,91						-2,99
AT5G02030	PNY	HB						0,65		-0,89
AT4G04890	PROTODERMAL FACTOR2 (PDF2)	HB		-1,43						-3,08
AT3G11260	WUSCHEL-related homeobox 5 (WOX5)	HB					1,72	-1,11		NA
AT4G35550	WUSCHEL-related homeobox 13 (WOX13)	HB		NA		0,87	0,91	NA	-0,76	
AT1G62990	KNAT7	HB					1,04		-1,11	
AT2G34710	PHABULOSA (PHB)	HB		-1,28			1,40	1,23	-1,22	0,86
AT5G45980	WUSCHEL-related homeobox 8 (WOX8)	HB						0,79	-1,23	
AT5G47370	HAT2	HB		-2,02	4,73				-1,73	1,41
AT5G20240	PISTILLATA (PI)	MADS					0,72		1,30	
AT5G13790	AGAMOUS-LIKE 15 (AGL15)	MADS						0,88		1,00
AT4G24540	AGAMOUS-LIKE 24 (AGL24)	MADS		-0,70						-1,06
AT2G03710	SEPALLATA4 (SEP4)	MADS		-0,80						
AT2G22540	SHORT VEGETATIVE PHASE (SVP)	MADS		-1,35		-0,66		0,50	-2,02	-3,03
AT5G23000	ATMYB37	MYB			-0,60					
AT1G52890	NAC4, ANAC019	NAC		4,52	-1,45			-0,75	-2,59	0,96
AT5G13180	VNDIP2, ANAC083, VNI2	NAC		1,60	-1,39					
AT1G01010	NAC1, ANAC001	NAC		1,47	1,83		-2,24		-1,36	
AT5G09330	ANAC082	NAC		0,86			NA	NA	NA	NA
AT2G18060	VASCULAR RELATED NAC-DOMAIN PROTEIN 1 (VND1)	NAC						0,50		
AT3G15510	ATNAC2, ANAC056, NARS1	NAC						0,56	-1,60	
AT1G53230	TCP3	TCP		-1,38			-0,72		1,01	-1,59
AT2G31070	TCP10	TCP		-0,80		0,85	1,25	0,54		1,73
AT5G11030	ABERRANT LATERAL ROOT FORMATION (ALF4)				0,76					0,91
AT2G42840	Protodermal factor 1			-2,78						-4,22
AT2G32550	Cell differentiation, Rcd1-like protein							0,60	0,90	1,15

Supplemental Table 9. Expression profiles of selected TFs involved in developmental processes.

AGI	Function
AT4G17880	MYC4, basic helix-loop-helix (bHLH)
AT1G77920	bZIP family transcription factor
AT5G53290	CRF3, ERF ethylene response factor
AT5G07580	ERF - ethylene response factor
AT1G28360	ERF12, ethylene response factor
AT2G16400	BELH7, homeodomain-containing protein
AT1G15580	IAA5
AT4G28640	IAA11
AT3G15540	IAA19
AT4G32280	IAA29
AT1G62990	KNAT7
AT2G42430	LBD16, LOB domain protein
AT3G58190	LBD29, LOB domain protein
AT5G60890	MYB34
AT5G59780	MYB59
AT1G80840	WRKY40
AT5G26930	Zinc finger (GATA type) family protein
AT1G74660	MIF1, zinc finger homeobox family protein

Supplemental Table 10. Transcription factors involved in lateral root initiation (Parizot et al., 2010) and deregulated in our study.

AGI	Function		Family	PO/ Pliv	P24/ P0	P48/ P24	P96/ P48	P168/ P96	C/ P168	C/ Pliv	Cluster	Asymetric division	Pericycle differential expression
AT1G03790	Zinc finger C-x8-C-x5-C-x3-H type family protein	SOM	C3H	1,01							Cluster 1		
AT1G18860	WRKY DNA-binding protein 61	ATWRKY61, WRKY61	WRKY	1,22							Cluster 1		
AT4G03160				1,18							Cluster 1		
AT1G30810	Transcription factor jumonji (jmj) family protein		Jumonji	0,95							Cluster 1		P
AT1G65040	RING/U-box superfamily protein			0,78						NA	Cluster 1		
AT4G26930	Myb domain protein 97	ATMYB97	MYB	0,72							Cluster 1		
AT5G61890	Integrase-type DNA-binding superfamily protein	AP2 domain-containing transcription factor family protein	AP2-EREBP	1,47						3,33	Cluster 1		P
AT2G03710	K-box region and MADS-box transcription factor family protein	SEP4, AGL3	MADS	-0,80							Cluster 2		
AT2G26580	Plant-specific transcription factor YABBY family protein	YAB5	C2C2-YABBY	-1,28						-1,71	Cluster 2		
AT1G07640	Dof-type zinc finger DNA-binding family protein	OBP2, AtDof1	C2C2-Dof	-1,22						-2,65	Cluster 2		P
AT4G17810	C2H2 and C2HC zinc fingers superfamily protein	ZFP12	C2H2	-1,99						-2,62	Cluster 2		
AT5G07690	Myb domain protein 29	PMG2, ATMYB29	MYB	-1,17						-2,19	Cluster 2		
AT1G74660	Mini zinc finger 1	MIF1	zf-HD	-1,12					1,84		Cluster 2		
AT1G09030	Nuclear factor Y, subunit B4	NF-YB4	CCAAT	-1,94						-1,29	Cluster 2		
AT5G15830	Basic leucine-zipper 3	ATBZIP3	bZIP	-1,34						-1,95	Cluster 2		
AT1G79430	Homeodomain-like superfamily protein	WDY, APL		-0,93						-1,50	Cluster 2		P
AT4G37750	Integrase-type DNA-binding superfamily protein	DRG, CKC1, ANT	AP2-EREBP	-1,03					1,37	0,89	Cluster 2		
AT2G38950	Transcription factor jumonji (jmj) family protein		Jumonji		0,61				-0,75		Cluster 3		
AT4G34590	G-box binding factor 6	ATB2, ATBZIP11, BZIP11, GBF6	bZIP		1,02				-0,73		Cluster 3		
AT4G26920	START (StAR-related lipid-transfer) lipid-binding domain	GLABRA2 RARTF family			-1,05					-2,79	Cluster 4		
AT5G49700	Predicted AT-hook DNA-binding family protein				-0,70						Cluster 4		
AT2G14760	Basic helix-loop-helix (bHLH) DNA-binding superfamily protein	bHLH084	bHLH		-0,73						Cluster 4		
AT5G26660	Myb domain protein 86	ATMYB4, ATMYB86	MYB		-0,69					1,29	Cluster 4		
AT5G23000	Myb domain protein 37	ATMYB37, RAX1	MYB		-0,60						Cluster 4		
AT1G03800	ERF domain protein 10	AtERF10	AP2-EREBP		-0,65				-0,78		Cluster 4		
AT5G66270	Zinc finger C-x8-C-x5-C-x3-H type family protein	Zinc finger (CCCH-type) family protein	C3H	1,73	-0,70		0,77		-1,24		Cluster 5		
AT1G62370	RING/U-box superfamily protein	Zinc finger (C3HC4-type RING finger) family protein		2,47	-3,04		0,75		-1,46		Cluster 5		
AT4G10150	RING/U-box superfamily protein	Zinc finger (C3HC4-type RING finger) family protein		3,31	-1,29		-1,35	-1,01			Cluster 5		
AT5G01380	Homeodomain-like superfamily protein	Transcription factor	Trihelix	2,83	-1,34				1,58	2,59	Cluster 5		P
AT4G15420	Ubiquitin fusion degradation UFD1 family protein	PRLI-interacting factor K		2,42		-1,06				1,38	Cluster 5		P
AT1G66390	Myb domain protein 90	PAP2, AtMYB90	MYB	2,33	-2,31						Cluster 5		
AT3G06490	Myb domain protein 108	BOS1, AtMYB108	MYB	1,07	-0,77						Cluster 5		
AT2G38250	Homeodomain-like superfamily protein		Trihelix	1,34	-1,20						Cluster 5		P
AT4G17800	Predicted AT-hook DNA-binding family protein			0,71	-0,73					NA	Cluster 5		P
AT2G22760	basic helix-loop-helix (bHLH) DNA-binding superfamily protein	bHLH019	bHLH	0,72	-0,60						Cluster 5		P
AT3G23250	Myb domain protein 15	ATMYB15, ATY19	MYB	2,95	-0,77	1,68		-1,34	-2,79		Cluster 5		P
AT4G21440	MYB-like 102	ATMYB102, ATM4	MYB	1,81	-1,47						Cluster 5		
AT2G33710	Integrase-type DNA-binding superfamily protein	AP2-EREBP	AP2-EREBP	2,25	-1,49	0,85			-0,84		Cluster 5	5	
AT2G14210	AGAMOUS-like 44	AGL44, ANR1	MADS	0,82	-1,05						Cluster 5		
AT5G20240	K-box region and MADS-box transcription factor family protein	PI	MADS				0,72		1,30		Cluster 7		
AT3G58190	Lateral organ boundaries-domain 29	LBD29, ASL16	LOB				1,17				Cluster 7	5	
AT3G18400	NAC domain containing protein 58	ANAC058	NAC				1,53		-0,97		Cluster 7		
AT2G47260	WRKY DNA-binding protein 23	ATWRKY23, WRKY23	WRKY				1,11	0,94	-1,70		Cluster 8		P
AT5G45980	WUSCHEL related homeobox 8	STPL, WOX8	HB					0,79	-1,23		Cluster 8		
AT2G18060	Vascular related NAC-domain protein 1	ANAC037, VND1	NAC					0,50			Cluster 8		
AT5G02030	POX (plant homeobox) family protein	PNY, BLR, BLH9, RPL, HB-6, VAN, LSN	HB					0,65		-0,89	Cluster 8		
AT1G21970	Histone superfamily protein	NF-YB9, EMB212, LEC1	CCAAT					0,69	-1,44		Cluster 8		
AT2G46590	Dof-type zinc finger DNA-binding family protein	DAG2, AtDof2,5	C2C2-Dof					0,78		1,28	Cluster 8		
AT3G61850	Dof-type zinc finger DNA-binding family protein	DAG1, AtDof3,7	C2C2-Dof					0,63		0,87	Cluster 8		
AT5G57390	AINTEGUMENTA-like 5	CHO1, AIL5	AP2-EREBP					1,21		1,99	Cluster 8		
AT2G42430	Lateral organ boundaries-domain 16	ASL18, LBD16	LOB	1,37			0,76	-0,63		2,52		5	P
AT3G05155	Major facilitator superfamily protein			1,27		-0,85							
AT1G68360	C2H2 and C2HC zinc fingers superfamily protein				3,00					3,10			
AT1G12980	Integrase-type DNA-binding superfamily protein	DRN, ESR1	AP2-EREBP			0,76	2,51	1,32	-3,46	0,85			
AT3G11260	WUSCHEL related homeobox 5	WOX5	HB				1,72	-1,11		NA			
AT1G29280	WRKY DNA-binding protein 65	ATWRKY65, WRKY65	WRKY					-0,83					
AT4G20970	Basic helix-loop-helix (bHLH) DNA-binding superfamily protein	bHLH162	bHLH				-0,86						
AT5G62470	Myb domain protein 96	ATMYB96, mybcov1	MYB				-1,48		2,05				
AT4G37650	GRAS family transcription factor	SGR7, SHR	GRAS	-0,98		NA		1,12					X
AT5G25890	Indole-3-acetic acid inducible 28	IAR2, IAA28	AUX/IAA	-1,20	-0,71				2,49				
AT3G10000	Homeodomain-like superfamily protein	EDA31	Trihelix	-1,60			0,71		1,56	1,01			
AT1G26310	K-box region and MADS-box transcription factor family protein	CAL1, AGL10, CAL	MADS	-2,64						-3,12			
AT1G68520	B-box type zinc finger protein with CCT domain	COL6	C2C2-CO-like	-3,02			-1,20			-4,45			

Supplemental Table 11. Transcription factor targets of LHP1 that were deregulated in our study.

	All	Up	Down	Cluster	ChromDB
Pliv/Pls	4	0	4	C1	7
P0/Pls	75	23	52	C2	15
P0/Pliv	60	19	41	C3	25
P24/P0	58	36	22	C4	7
P48/P24	15	10	5	C5	9
P96/P48	27	17	10	C6	7
P168/P96	18	14	4	C7	2
C/P168	73	49	24	C8	6
C/Pliv	96	72	24	others	30
				Total	108

Supplemental Table 12. Distribution of the 559 ChromDB genes deregulated in our study and in the eight main clusters.

Cluster	AGI	Function	ChromDB ID/formal name	1	2	3	4	5	C/ P168 6	C/ Pliv 7	8	9
Cluster 10	AT2G27880	Argonaute family protein	AGO5									
	AT5G22750	DNA/RNA helicase protein	CHR29									
	AT5G15380	DNA methyltransferases	DMT9/DRM1									
	AT3G62800	Double-stranded-RNA-binding protein	DRB4									
	AT3G58780	Transcription factor family protein	FLCP24/SHP1									
	AT5G23260	Transcription factor family protein	FLCP7/TT16									
	AT5G08565	Global transcription factor group	GTG2									
	AT1G20693	HMG group family	HMGB2									
	AT4G35570	HMG group family	HMGB5									
	AT3G24010	RING/FYVE/PHD zinc finger superfamily protein	INGF1									
	AT1G23230	Mediator subunit	MED23SUB1									
	AT2G03070	Mediator subunit	MED8SUB1									
	AT4G35050	NURF complex component	NFC3/MSI3									
	AT5G17240	SET domain protein	SDG40									
	AT1G49950	Single myb histone protein group	SMH10/TRB1									
	AT4G02730	COMPASS complex	SWDC1									
	AT5G25150	TBP-associated factor	TAFV1/TAF5									
Cluster 11	AT2G36490	Superfamily of DNA glycosylases	DNG1/ROS1									
	AT3G20810	Jumonji domain group	JMJ30									
	AT4G22745	Methyl-CPG-binding domain protein	MBD1									
Cluster 12	AT3G57230	Transcription factor family protein	FLCP17/AGL16									
	AT3G18520	Histone deacetylase	HDA15									
	AT2G17560	HMG group family	HMGB4									
	AT5G02850	hydroxyproline-rich glycoprotein family protein	MED4SUB1									
	AT1G65470	Nucleosome/chromatin assembly complex protein	NFF2/FAS1									
	AT5G45600	YEATS family protein	YDG1/GAS41									
Cluster 13	AT3G43920	Dicer-like group	DCL3									
	AT3G27000	Actin related protein 2	ARP2/WRM									
	AT4G10050	esterase/lipase/thioesterase family protein	ABHF7									
	AT1G76710	SET domain protein	SDG26/ASHH1									
	AT5G23405	HMG group family	HMGB12									
	AT5G20170	Mediator subunit	MED17SUB1									
	AT3G52860	Mediator subunit	MED28SUB1									
	AT4G20910	HUA Enhancer	HEN1									
	AT2G28290	SNF2 super family	CHR3/SYD									
	AT5G48600	Structural maintenance of chromosome 3	CPC1/SMC4									
	AT3G01770	Global transcription factor group	GTE11/ATBET10									
	AT5G14270	Global transcription factor group	GTE9									
	AT5G09740	Histone acetyltransferase of the MYST family 2	HAM2									
	AT5G04240	Jumonji domain group	JMJ11/ELF6									
	AT4G04780	Mediator subunit	MED21SUB1									
	AT1G65440	Global transcription factor group	GTB1									
	AT1G16710	Histone acetyltransferase	HAC12									
	AT2G45640	Sin3 complex component	HCP1									
	AT5G14530	COMPASS complex	SWDB1									
Cluster 14	AT1G48410	Argonaute gene family	AGO1									
	AT5G24930	Transcription factor family protein	CONS5/COL4									
	AT5G10140	Transcription factor family protein	FLCP1/FLC									
	AT2G45660	Transcription factor family protein	FLCP29/AGL20									

Supplemental Table 13. The ChromDB genes deregulated in *A. thaliana* cell suspension form five new clusters.

AGI	Family	Tag DE5	P0/ Pliv	P24/ P0	P48/ P24	P96/ P48	P168/ P96	C/ P168	C/ Pliv
AT1G62230	Pseudogene	DE5							
AT4G37620	Other	DE5							
AT2G05935	Non-LTR	DE5							
AT2G09860	Non-LTR	DE5							
AT1G67240	Mutator-like	DE5							
AT2G13850	Copia-like	DE5							
AT2G07090	Other	DE5							
AT4G10990	Copia-like								
AT1G06740	Mutator-like								
AT5G35720	Non-LTR								
AT5G30460	Pseudogene								
AT2G10410	Sadhu								
AT2G12020	Gypsy-like								
AT1G21220	Copia-like								
AT3G42622	Gypsy-like								
AT1G43725	Copia-like								
AT3G42792	Mutator-related								
AT5G27345	Mutator-like								
AT2G04460	Other								
AT3G24675	Non-LTR								
AT2G16140	Other								
AT1G35110	Other								
AT4G18410	Mutator-like								
AT1G12720	Mutator-like								
AT1G43930	Mutator-like								
AT1G43886	Copia-like								
AT2G07630	Other								
AT2G11150	Replication								
AT5G10850	Other								

Supplemental Table 14. Expression profiles of transposable elements during *A. thaliana* protoplast culture compared to cell suspension (C) culture.

SUPPLEMENTAL METHODS

CATMA transcriptome hybridization and data analysis

For each CATMA array comparison, one technical replicate with fluorochrome reversal was performed for each biological replicate (i.e., four hybridizations per comparison). The labeling of complementary RNAs with Cy3-dUTP or Cy5-dUTP (Perkin-Elmer-NEN Life Science Products), hybridization to the slides, and scanning were performed as described previously (Lurin et al., 2004). For each microarray analysis, the raw data comprised the logarithm of the median feature pixel intensity at wavelengths 635 nm (red) and 532 nm (green).

Statistical Analysis of Microarray Data

The normalization and statistical analysis were based on two dye swaps (i.e., four arrays) per comparison (Gagnot et al., 2008). An array-by-array normalization was performed to remove systematic biases. Spots considered as badly formed features were excluded from the analysis. A global intensity-dependent normalization using the loess procedure (Yang and Thorne, 2003) was then performed to correct for dye bias. Finally, for each block, the log-ratio median calculated over the values for the entire block was subtracted from each individual log-ratio value to correct print-tip effects. Differential analysis was based on the mean log ratios of the dye-swap analysis of each biological replicate. These technical replicates were thus averaged to derive one log-ratio per biological replicate, and the values obtained were then used in combination to perform a paired t-test for each set of biological replicates. In this test, the variance modeling was a trimmed variance, calculated from genes that do not display extreme variance. The genes excluded were those with a specific variance/common variance ratio smaller than the alpha-quantile or greater than the (1-alpha)-quantile of a chi-squared distribution with two degrees of freedom and an alpha = 0.0001. The raw P-values obtained were adjusted by the Bonferroni method, which controls the Family Wise Error Rate (Ge et al., 2003), to strongly limit false positives in a multiple comparison context. Genes with a Bonferroni P-value of < 0.05 were considered to be differentially expressed (Gagnot et al., 2008).

Quantitative real-time RT-PCR

Reverse transcription (RT) reactions were performed with Superscript II reverse transcriptase (Invitrogen) according to the manufacturer's instructions. Quantitative real-time RT-qPCR was performed in an Eppendorf Mastercycler® ep realplex (Eppendorf) using ABI PRISM 7900HT

(Applied Biosystem) with MESA FAST qPCR MasterMix Plus for SYBR® Assay (Eurogentec) as per manufacturer's instructions.

The results of three technical replicates of two biological samples were normalized with *AIA12* which showed a steady level of transcription. The following primer pairs were used:

AIA12 (5'ACGTCAAGAGCAGAAGGATAGA3'; 5'AACAAGAGCTTTCTCTCACAG3')

ANAC042 (5'TCCAACTTGCTGAGTCTCC3'; 5'GCAGCTTAGATTCCGACCA3');

ANAC003 (5'ACCATGTTTCCCATTCCTCA3'; 5'TCCTCACTTCACAGAGAAGATCC3');

KPR6 (5'ACGAACTGTTCTTCGCGATT3'; 5'TCTTCGCGGTTTCATCTTCT3');

KPR1 (5'ACACGACTTTTCTGGGCTCT3'; 5'GCCATTAGAAGGACGTTACGA3');

TtsZ (5'GGAGACTGCTTCTGGTGAGG3'; 5'ACAAGTTTGGCAGACCCATC3');

ESR1 (5'TGCCTGGAACCAAGGTTTTCT3'; 5'GGCGTCGCGTAAGAAGATAG3');

CYCD21(5'CATGACTCAACTGTTCTCTCTTCA3';
5'AGAAGTCTCACTGGGGAGGAG3');

SKIP1 (5'AAACAACCGACCCAAGTCAG3'; 5'CAAGGTCAGGGGATGTGG3').

SUPPLEMENTAL REFERENCES

Breeze, E., et al. (2011). High-resolution temporal profiling of transcripts during Arabidopsis leaf senescence reveals a distinct chronology of processes and regulation. Plant Cell 23: 873–894.

Damri, M., Granot, G., Ben-Meir, H., Avivi, Y., Plaschkes, I., Chalifa-Caspi, V., Wolfson, M., Fraifeld, V., and Grafi, G. (2009). Senescing cells share common features with dedifferentiating cells. Rejuvenation Res. 12: 435–443.

Gamborg, O.L., Miller, R.A., and Ojima, K. (1968). Nutrient requirements of suspension cultures of soybean root cells. Exp. Cell Res. 50: 151–158.

Gagnot, S., Tamby, J.-P., Martin-Magniette, M.-L., Bitton, F.,Taconnat, L., Balzergue, S., Aubourg, S., Renou, J.-P.,Lecharny, A., and Brunaud, V. (2008). CATdb: A public access to Arabidopsis transcriptome data from the URGV-CATMA platform.Nucleic Acids Res. 36 (Database issue): D986–D990.

Ge, Y., Dudoit, S., and Speed, T.P. (2003). Resampling-based multiple testing for microarray data analysis. TEST 12: 1–44.

Heller, R. (1953). Recherches sur la nutrition minérale des tissus végétaux cultivés in vitro. Ann. Sci. Nat. Bot. Biol. Veg. 14: 1–223.

Lurin, C., et al. (2004). Genome-wide analysis of Arabidopsis pentatricopeptide repeat proteins reveals their essential role in organelle biogenesis. Plant Cell 16: 2089–2103.

Morel, G., and Wetmore, R.H. (1951). Fern callus tissue culture. Am. J. Bot. 38: 141–143.

Murashige, T., and Skoog, F. (1962). A revised medium for rapid growth and bioassays with tobacco tissue cultures. Physiol. Plant.15: 473–497.

Parizot, B., De Rybel, B., and Beeckman, T. (2010). VisuaLRTC: A new view on lateral root initiation by combining specific transcriptome data sets. Plant Physiol. 153: 34–40.

Roscoe, D., and Bell, G. (1981). Use of pH indicator in protoplast culture medium. Plant Sci. Lett. 21: 275–279.

Yang, Y.H., and Thorne, N. (2003). Normalization for two-color cDNA microarray data. In Science and Statistics: A Festschrift for Terry Speed, IMS Lecture Notes, Monograph Series, Vol. 40, D.R. Goldstein, ed (Beachwood, OH: Institute of Mathematical Statistics), pp. 403–418.

Yadav, R.K., Girke, T., Pasala, S., Xie, M., and Reddy, G.V. (2009). Gene expression map of the Arabidopsis shoot apical meristem stem cell niche. Proc. Natl. Acad. Sci. USA 106: 4941–4946.

Xiao, L., Zhang, L., Yang, G., Zhu, H., and He, Y. (2012). Transcriptome of protoplasts reprogrammed into stem cells in Physcomitrella patens. PLoS ONE 7: e35961.